scientific reports

Check for updates

OPEN

A melanin-like polymer bearing phenylboronic units as a suitable bioplatform for living cell display technology

Danilo Vona[1,6], Stefania Roberta Cicco[2,6], Cesar Vicente-Garcia[3], Alessandro Digregorio[3], Giorgio Rizzo[3], Rossella Labarile[4], Maria Michela Giangregorio[5], Carlo Porfido[1], Roberto Terzano[1], Emiliano Altamura[3], Pietro Cotugno[3]✉ & Gianluca Maria Farinola[3]

Surface display of functional groups with specific reactivity around living cells is an emerging, low cost and highly eco-compatible technology that serves multiple applications, ranging from basic biochemical studies to biomedicine, therapeutics and environmental sciences. Conversely to classical methods exploiting hazardous organic synthesis of precursors or monovalent functionalization via genetics, here we perform functional decoration of individual living microalgae using suitable biocoatings based on polydopamine, a melanin-like synthetic polymer. Here we demonstrate the one-pot synthesis of a functional polydopamine bearing phenylboronic units which can decorate the living cell surfaces via a direct ester formation between boronic units and surface glycoproteins. Furthermore, biosorption of fluorescent sugars on functionalized cell membranes is triggered, demonstrating that these organic coatings act as biocompatible soft shells, still functional and reactive after cell engineering.

Keywords Organic biopolymers, Polydopamine, Boronic acid, Polysaccharides, Living materials, Organic coatings

Living cells can act as natural platforms displaying various functional groups or biomolecules. The introduction of an engineered chemical surface over living cells allows bacteria, mammalian and human cells, yeasts and microalgae to recognize their environment and integrate cell:cell and cell:environment interactions. An exogenous functional group grafted on the surface of living cells can lead to the production of biohybrids useful for different applications ranging from immunotherapy[1], tissue engineering[2], to stem cell confining[3]. Functionalization methods have historically been developed for monovalent functionalization, using expensive genetic engineering or biorthogonal click chemistry[4]. The latter chemical methodology is quite laborious since it consists of a metabolic insertion of first hit molecular precursors followed by an external click reaction, also recently optimized to improve polyvalent and multifocal surface display of functional groups or biomolecules on living cells[5,6] or extracts[7]. These techniques include ad hoc new synthesis building blocks [8,9] followed by azide-alkyne or strains promoting cycloaddition and Staudinger ligation reactions[10]. In all these cases, the chemical methodologies are performed to decorate, label, trigger or investigate the living cell surfaces. These outcomes ideally occur without affecting the cell viability[11] or metabolic activity, while always ensuring a biologically benign character, rapid reaction rates under physiological conditions and the generation of non-toxic side products. Unfortunately, the click chemistry hides the underestimated risk of difficult, serial and time/energy consuming preparation of all the small organic precursors. Here we tile for the first time the prospect of universally decorating living cells with melanin-like sticky organic polymers, bearing exogenous boronic acid units which dramatically change the chemical reactivity on the living cell surfaces. Polydopamine (PDA), a poly-hydroxy-indole specie, has recently been considered as an organic polymer with unique and universal coating properties to give living microalgae

[1]Dipartimento Di Scienze del Suolo, Della Pianta E Degli Alimenti (Di.S.S.P.A.), Università Degli Studi Di Bari "Aldo Moro", Via G. Amendola 165/A, 70126 Bari, Italy. [2]Consiglio Nazionale Delle Ricerche, CNR-ICCOM, Via E. Orabona 4, 70126 Bari, Italy. [3]Dipartimento Di Chimica, Università Degli Studi Di Bari "Aldo Moro", Via E. Orabona 4, 70126 Bari, Italy. [4]Consiglio Nazionale Delle Ricerche, IPCF-CNR, Via E. Orabona 4, 70126 Bari, Italy. [5]Institute of Nanotechnology, CNR-NANOTEC, Via Orabona 4, 70126 Bari, Italy. [6]These authors contributed equally: Danilo Vona and Stefania Roberta Cicco. ✉email: pietro.cotugno@uniba.it

cells the capability to both continue living/dividing, increase cell resistance under harsh environmental conditions and catching pollutants[12]. In count, the PDA biocompatibility has been proven on intact bacterial cells[13], on photosynthetic proteins that retain their photoactivity[14] thus making it suitable for sensing applications.[15,16] Also, PDA has always attracted material scientists for its envisaging application in biomedicine, and generally melanin-like polymers are showing nowadays applicability also for potential clinics and therapeutics. By a chemical point of view[17], dopamine monomer (DA) self-polymerizes readily in presence of oxygen under mild alkaline conditions. The resulting polymerization leads to adherent layers of PDA with characteristic inducible conductive properties[18]. Here we exploit the co-polymerization of DA with 3-aminophenylboronic acid (APBa) in ammonia solution. After the physico-chemical characterization of the polymer, different cell lines were coated with this boronic-bearing luminescent polymer, demonstrating its intrinsic capacity to target microalgae cells which exhibit high density glycocalyx. We furthermore exploited the residual free boronic units of the decorated living cells to nano-aggregate sugar-based biomolecules, such as 5(6)-isothiocyanate-dextran (FITC-DX) on cell surfaces, which easily act as living platforms displaying chemical moieties (Fig. 1).

Methods

Materials Tris·HCl, dopamine·HCl 98%, 3-aminophenylboronic acid (APBa), 3-aminomethylphenylboronic acid, 3-mercaptophenylboronic acid (MPBa), phenylboronic acid (PBa), 3-carboxyphenylboronic acid (CPBa), fluorescein isothiocyanate-dextran (FITC-DX), diatomaceous earth (silica microparticles), Alizarin Red S (ALI), Cyanine-3-N-hydroxysuccinimidyl-estere (Cy3-NHS) were purchased from Sigma Aldrich St. 4,7-di(thiophen-2-yl)benzo[1,2,5]thiadiazole (T-BTZ-T) was obtained via synthetic route using a literature procedure[8].

Equipment Raman spectra were collected using a LabRAM HR (Horiba-Jobin Yvon, Montpellier, France) spectrometer with 532 nm excitation laser under ambient conditions. Low laser power (< 1 mW) was used to avoid heat-induced modification or degradation of the sample due to focused laser light during spectrum acquisition. The collection time was longer than 200 s. The excitation laser beam was focused through a 50X optical microscope (spot size ~1 cm, and working distance 1 cm). The spectral resolution was 1 cm^{-1}[15]. Raman measurements were used to detect vibrational bonds between B, C and O atoms and to obtain a fingerprint of the molecule. Confocal imaging was performed with a Leica SP8 X (bright field, fluorescence function, 3D and merge mode) laser scanning confocal microscopy. Bright-field optical images/bidimensional fluorescence images were recorded in reflection, using Axiomat microscope, Zeiss. Fourier Transformed Infrared-Attenuated Total Reflectance (FTIR-ATR) spectra were acquired with a Perkin Elmer Spectrum Two Spectrophotometer equipped with A 2 × 2 mm diamond crystal. Spectra were recorded in the range 4000–400 cm^{-1} with a 2 cm^{-1} resolution, using 0.25 cm^{-1} acquisition interval and acquiring 32 scans for each sample[21]. High-resolution mass spectra were recorded by a Shimadzu high-performance liquid chromatography-ion trap-time of flight mass spectrometer (LCMS-IT-TOF). ^{1}H NMR and ^{13}C NMR spectra were recorded at 500 MHz and 125 MHz, respectively, using an Agilent Technologies 500/54 Premium Shielded spectrometer. For TXRF technique, samples were analyzed for 1000 s using a S2 Picofox Spectrometer (Bruker Nan GmbH, Berlin; Germany) equipped with a Mo microfocus tube (30 W, 50 kV, 600 µA), a multilayer monochromator, and an XFlash® silicon drift detector with a 30 mm^2 active area. The energy resolution, measured at the Kα of Mn, was b150 eV (10 kcps).

Synthesis of PDA-APBa (1) in ammonia solution

The dopamine (DA) monomer (1 mmol) was poured in 5 mL of a solution containing 1% ammonia (V/V) in water and stirred for 15' at room temperature. Then 1 mL of bidistilled water containing 1% ammonia with

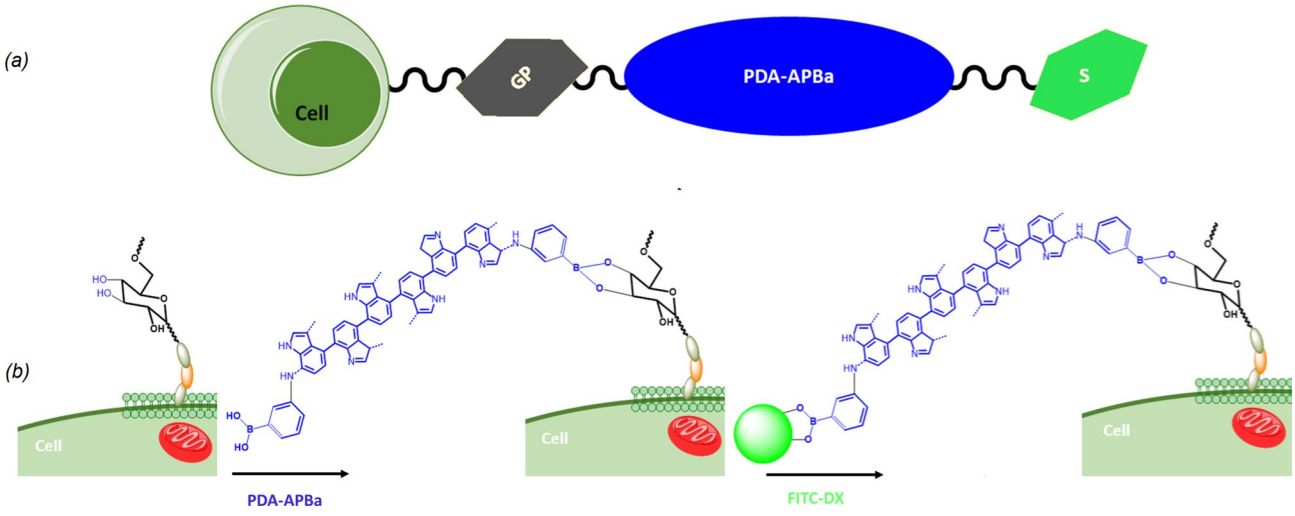

Figure 1. Representative scheme of PDA-APBa grafting on living cells and reacting with labelled water soluble polysaccharides. (**a**) The dopamine-3-aminophenylboronic acid (PDA-APBa) polymer acts as a cross-linker between living cells, directly anchoring glycoproteins (GP), and further saccharides units (S). (**b**) Details of the direct ester formation between boronic units and surface glycoproteins and consequent ester formation between boronic units and the fluorescently labelled 5(6)-isothiocyanate-dextran (FITC-DX).

1 mmol APBa (from acetone stock, 0.2 mL) was added dropwise. The reaction was kept at room temperature, under stirring, for 24 h. An orange-reddish polymer, still soluble in the reaction vessel, appeared after 3–4 h of reaction. Then the solution was quenched with 2 mL HCl 1 M, the solvent was vacuum assisted evaporated, and different washing steps with hot acetone were performed to purify the polymer from the unreacted monomers. The precipitate was re-collected in bidistilled water.

Synthesis of PDA-mPBA (2), PDA-PBA (3), and PDA-CPBa (4)

The DA monomer (1 mmol) was poured in 5 mL of water solution containing 1% ammonia and stirred for 15' at room temperature. Then 1 mL of bidistilled water with 1 mmol of mPBA or PBA or CPBa (from acetone stock, 0.2 mL) was added dropwising. The reaction was kept at room temperature, under stirring, for 24 h. Brown or dark polymers appeared and precipitated after 3–4 h of reaction. Then the solution for each polymerization reaction was quenched with 2 mL HCl 1 M, and an enhanced precipitation was obtained treating with 6 mL of acetone at 4 °C for 24 h. The precipitate was recollected. Control reactions were performed with dopamine alone and 3-aminophenylboronic acid alone, under the same polymerization conditions. Only the first reaction yields to polydopamine, while no reaction occurred in the case of APBa monomer.

Polymerization of dopamine in ethanol

The dopamine polymer powder (14.5 mg) was poured in 5 mL of pure ethanol and stirred for 15' at room temperature. Then pyridine (0.35 mL) was added dropwise in 5 mL of ethanol solution (Liu et al., 2018). After 12 h reaction, the solvent was vacuum pumped and the precipitate washed with a solution 1:1 ethyl ether: ethyl acetate to remove pyridine, water and unreacted DA monomer and oligomers. The remaining PDA precipitate was solubilized in MetOD and investigated via ^{1}H-NMR and ^{13}C-NMR, to be compared with PDA:APBa co-polymer (dissolved in D_2O). Moreover, the presence of characteristic dimers was investigated using the washing organic layers obtained from the polymer precipitate, via LC–MS.

Co-polymerization of dopamine and 3-aminomethylphenylboronic (AMPBa) acid in ammonia solution

A derivative phenylboronic acid (3-aminomethylphenylboronic, AMPBa), characterized by the presence of an amino-group indirectly linked to phenyl unit via a methyl-bridge, has been tested for dopamine co-polymerization. As expected, a low fluorescent co-polymer with very low solubility was obtained, maybe due to the absence of a direct *aromatic* C-N-*aromatic* C bond which likely causes the rise of the fluorescent properties in the case of the PDA-APBa co-polymer.

Reporting the synthetic route, DA (1 mmol) was poured in 5 mL of a water solution containing 1% ammonia and stirred for 15' at room temperature. Then 1 mL of bidistilled water containing 1% ammonia with 1 mmol AMPBa (from acetone stock, 0.2 mL) was added dropwising. The reaction was kept at room temperature, under stirring, for 24 h. An orange-reddish polymer, still soluble in the reaction vessel, appeared after 3–4 h of reaction. Then the solution was quenched with 2 mL HCl 1 M, the solvent was vacuum assisted evaporated, and different washing steps with hot acetone were performed to purify the polymer from the unreacted monomers. The precipitate was re-collected in bidistilled water.

Catching of FITC-DX via functionalized microparticles

An experiment of FITC-DX catching by PDA-APBa coated silica microparticles (diatomaceous earth, Sigma Aldrich, 1 mg) has been carried out, leading to a trapping of 19% of FITC-DX from a solution containing 1 mM of the fluorescently labelled polysaccharide. This outcome has been demonstrated more efficient than the catching performed by the lone silica microparticles (1 mg, 4%) and the silica microparticles coated with the lone PDA (6%).

Investigation of microalgae nutrients via total reflection X-ray fluorescence spectrometry (TXRF)

Data of nutrients uptake from living *Chlorella vulgaris* microalgae, with and without polymer **1** organic coatings, have been registered and exploited here as a novel data tool to define cell viability. Bare and coated samples were immersed for 6 days in their enriched semi-artificial microalgae medium, to enable living cells catch nutrients from the solutions. Then microalgae were collected (3000 rpm, 15'), washed 5 times with bidistilled water, and 2–3 mm diameter films were drop casted over plexiglass round disks. Casted films have been obtained starting from 7 10^6 dense cell suspensions (0.1 mL bd water), reaching a dried film mass of 0.300 mg for bare cells and 0.360 mg for coated cells. These samples were analyzed by total reflection X-ray fluorescence spectrometry (TXRF) for detecting nutrients concentration. Sample preparation was adapted from Allegretta et al.[19]. Briefly, 5 µl of 1000 mg/L V standard solution (Sigma-Aldrich) was mixed with 80 µl of each sample; after vortexing for 15 s, 10 µl of sample was deposited on a clean plexiglass reflector and left until complete dryness on a heating plate set at 50 °C under laminar flow hood.

Preparation of samples for bidimensional and confocal microscopies

Each sample, bare (without polymer and without FITC-DX), after polymer **1** treatment and after FITC-DX incubation, has been washed with buffer solution (Tris:HCl 20 mM, pH 7.4, waterish buffer) and spotted on glass slides, and observed both in wet and dried state, in comparison with control samples. Bidimensional microscopy was performed using DAPI passband filter for polymer **1** observation, and FITC passband filter for FITC-DX

investigation. Confocal microscopy was used recurring to λexc.: 405 nm/λem.: 477 nm for polymer **1** imaging, and λexc.: 488 nm; λem.: 521 nm parameters for FITC-DX observation.

Results and discussion

A new organic polymer based on polydopamine, and containing active boronic units, is proposed in this work for the first time. Our investigation de facto begins with the use of green, one-pot chemistry to synthesize a polyhydroxy-indole bulk modified with phenyl boronic moieties. This synthesis starts recurring to a co-polymerization of dopamine monomer with boronic aromatic species bearing specific functional groups directly addressing dopamine, such as free amines or thiols. Based on a co-polymerization protocol[20], 3-aminophenylboronic acid (APBa, Fig. 2a, polymer **1**) and other related chemicals (3-mercaptophenylboronic acid, MPBa; phenylboronic acid, PBa; 3-carboxyphenylboronic acid, CPBa; Fig. 2a 2–4, respectively), have been considered for dopamine functionalization during its first oxidative conversion step, using a solution of 1% ammonia in bidistilled water, at room temperature, under stirring, for 24 h (Supplementary Information (SI) section for control reactions). Among all the attempted reactions, only output **1** gave a water soluble polymer. Furthermore, polymer **1** exhibits high fluorescence intensity when excited at 375 nm (emission wavelength, 497 nm) in water (Figure S1). Polymer **1** was first characterized in solid phase, using FT-IR spectroscopy (Fig. 2b) and Raman Spectroscopy (Fig. 2c–e). Together with the lone dopamine polymerization control (Figure S2), a further control reaction has been introduced in this work exploiting a phenylboronic unit with amino-group indirectly linked via a methyl function (Figure S3 and comments). The comparison between the FT-IR spectrum of PDA-APBa, those of PDA monomers and free APBa (Fig. 2b), evidenced the presence of a sharp signal at 1395 cm^{-1}, attributable to the B-O stretching vibration. Moreover, multiple serial signals after 1900 cm^{-1} underline the presence of the overtones related to the aromatic rings.[21] Fig. 2c–e shows Raman spectra of PDA films drop casted on silicon before (PDA) and after co-polymerization with 3-aminophenylboronic acid (PDA-APBa), compared again with the Raman spectrum of the reference 3-aminophenylboronic acid (APBa). Raman spectra in the wide range, 100–1000 cm^{-1} (Fig. 2d), are dominated by a very intense band at ~485 cm^{-1} due to C–C–C–C torsion (Γ_{CCCC}) hiding weaker Raman signals. To highlight them, Raman measurements have been also performed in two zoomed ranges, 70–450 cm^{-1} (Fig. 2c) and 500–1000 cm^{1} (Fig. 2e). Raman spectra of pure PDA (black lines) show bands corresponding to vibrational frequencies of bonds between C and C, O, H and N atoms, while the Raman spectra of the reference 4-aminophenylboronic acid (green lines) shows bands corresponding to vibrational frequencies of bonds between B, C and O atoms[22,23].

After doping with 3-aminophenylboronic acid (PDA-APBa, red lines), the Raman spectra of PDA change, showing the presence of additional peaks, evidenced by red asterisks, due to the formation of bonds between B, C and O (see Fig. 2c and e), in both measurement ranges. Raman characterization has also been extended to wavenumbers higher than 1000 cm^{-1} as shown in Figure S4, confirming the efficacy of the PDA doping with 3-aminophenylboronic acid. Going over the investigation and for an insight into the structure, polymer **1** dissolved in D_2O was characterized by using ^{1}H-NMR and ^{13}C-NMR. These methods were used to record spectra of PDA-APBa for comparison with those of lone soluble PDA, obtained using pyridine catalyst (section S2)[23] and APBa monomer. An important and common group of signals ranging from 6 to 7.6 ppm in the ^{1}H spectrum was assigned to the aromatic protons for both PDA and PDA:APBa. A last set of signals appearing from 8 to 8.6 ppm was assigned to hydroxyl protons of catechol moieties. In the ^{1}H-NMR spectrum belonging to PDA:APBa the presence of multiplets at 7.05 and 7.45 reflected the presence of the APBa moieties[24], whose spectrum is magnified in the inset of Figure S5. The ^{13}C-NMR spectrum of the boronic-functionalized polymer (Figure S6, in dark red) shows chemical shift signals set around 161–163 ppm, corresponding to carbonyl carbon atoms from the quinone present in the polymer structures. Signals at 119, 121 and 125 ppm belong to carbon atoms of aromatic moieties present in the lone APBa molecule and in the proposed co-polymer. Lone PDA was not solved in ^{13}C NMR experiment due to its low solubility. The presence of characteristic DA-APBa dimers (285.0821 Da, Figure S7) in the organic layers deriving from the washing steps of the co-polymer, has been recorded via high resolution LC–MS (Chan, 2019). PDA shows DA-DA dimer set around 293.113 Da. The fragmentation profile of the dimer has been reported in Figure S8.

The chemical characterization of the proposed polymer gave enough information about structure, monomer repetition, spectroscopic and optical features and the presence of active boronic species. This new synthesis of boronic-bearing polymer **1** is intended to be exploited to directly address living cells in cell media, keeping it stable in contact with water, waterish media and biological matrices. The addressing of polymer **1** aims to occur on sugar moieties of living cells. This should be done in principle via the esterification reaction of the boronic unit with the vicinal diol functionalities of the saccharides on living cell surface. The two scenarios for obtaining this functionalization are: (i) the co-polymer production directly around living cells, by incubating these biological partners with the monomers, and (ii) the incubation of living cells with the preformed polymer 1. Unfortunately, changing the conditions of the polymerization reaction and, specifically, avoiding the use of ammonia and performing the polymerization of dopamine and APBa in biocompatible media (sea water, Tris:HCl, Tris(hydroxymethyl)aminoethane and Dulbecco's modified Eagle Medium (DMEM)), the resulting polymer presents low solubility in water and in many organic solvents , with no fluorescence emission. The ^{1}H-NMR spectra of polymer **1**, synthesized from dopamine and APBa, in sea water, Tris:HCl and DMEM, are reported in Figure S9. As shown in the latter figure, a lack of peculiar signals from the APBa inner moiety is evident in the spectra.

After the polymer structure characterization, the amount of phenylboronic units into PDA-APBa has been quantified by a titration in solution with increasing amounts of Alizarin Red S (ALI, Figure S10)[25], a reagent specifically used to form catechol:boronic interaction with phenyl-boronic derivatives. ALI interaction with PDA-APBa leads to fluorescence quenching, directly proportional to the reagent amount. After the titration,

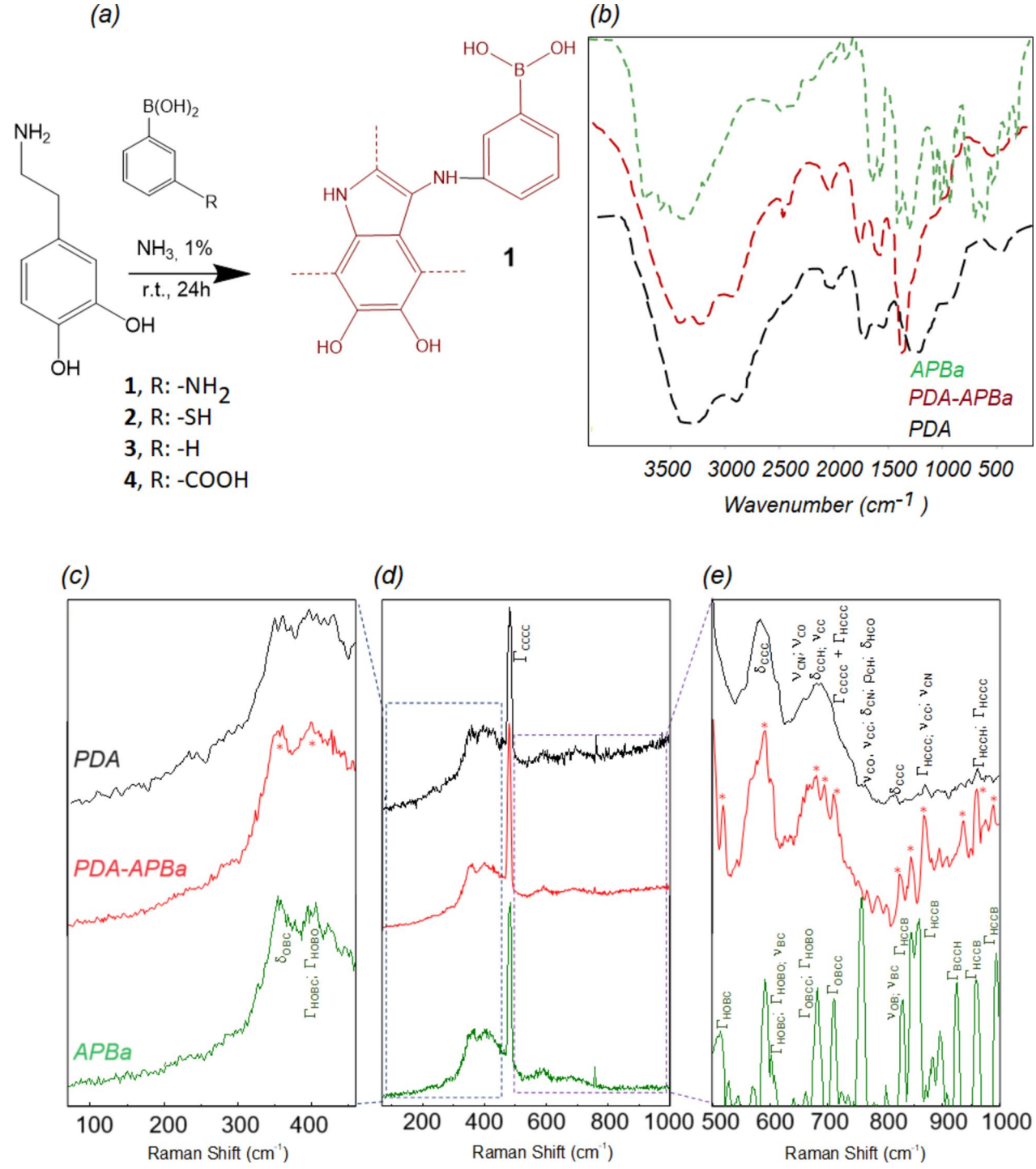

Figure 2. (**a**) Co-polymerization of R-arene species and dopamine; (**b**) FT-IR characterization of PDA-APBa in comparison with APBa and PDA; (**c**–**e**) Raman spectroscopy characterization of PDA-APBa in comparison with APBa and PDA. Red asterisks in the Raman spectra of PDA-APBa films indicate the formation of B-C/B-O modes, not present in pure PDA. Raman vibrations, (torsion), (bending), (stretching) and (rocking) are also specified.

0.504 mg of ALI were consumed to quench 0.1 mg of PDA-APBa, underlining the presence of 14 μmol of -$B(OH)_2$ per mg of the polymer.

Resilient, sugar-enriched, living marine microalgae were chosen here to perform the biological experiments with the polymer **1**, aiming to find the best combination in terms of cells viability, surface addressing and polymer bulk concentration in waterish stocks. The following microalgae cells, exhibiting a plethora of glycoproteins and membrane-associated polysaccharides, have been exploited here as living platforms: *Dunaliella tertiolecta* (D) and *Chlorella vulgaris* (C) as green microalgae, *Thalassiosira weissflogii* (T) and *Navicula pelliculosa* (N) as

model diatoms. For the biological approaches and investigations, all these cells were incubated with polymer **1** at the concentration of 0.1 mg/mL in sea water for 1 h, 4 h and 24 h (Figures S11–S12). As expected, *Dunaliella tertiolecta* did not exhibit any blue fluorescence signal due to the low density of glycoproteins on cell surface, while *Navicula pelliculosa* accumulates the emitting polymer between cell structures, underlying that it links to the extracellular polysaccharide matrix (EPS). In this case N cells do not act as living platforms, because the saccharide units are not uniformly distributed over the cell surface, however the polymer successfully addressed these functionalities in EPS. T cells often internalize the polymer, maybe due to serial processes of passive surface interaction and active cell uptakes. This internalization phenomenon can be also due to the natural degradation of the external T cell membranes, leading to an inner accumulation and a cytoplasmic addressing of the polymer **1**. The best candidate in terms of cell surface glycoprotein distribution is *Chlorella vulgaris*, as reported in the literature[26], thus reflecting a uniform coating with the emissive polymer **1**. In this case the boronic unit provokes a direct condensation reaction with 1,2- or 1,3-diol groups, typical of mono-, di- and polysaccharides both in extracts and living cells. This click reversible reaction requires mild experimental conditions (pH 7–8) with a pH-dependent reversibility, allowing a better, fast control of the attachment/detachment process[27]. These receptor:ligand-like interactions have been also exploited in the production of surface devices for mammal cell adhesion, attachment and recognition, till the final modulated release[28]. In this case, the interaction of boronic free units and aromatic catechol (in DOPA moiey) of specific peptides has been utilized, leading to the formation of a dynamic catechol:phenyl boronic cyclic ester functional to the tuning of cell attachment and cell migration[29]. Our polymer, containing covalently bound phenylboronic units, best performs at a contact concentration of 0.5 mg/mL (Figure S13). As shown in Fig. 3 (Figure S15 for 3D reconstruction), chloroplasts appear huge, round, strongly red emitting, and the polymer signals (blue emission) seem to perfectly profile the cell surfaces. The merge mode evidenced the absence of a co-localization between the two fluorescence signals. Coated living cells have been, then, incubated with FITC-DX as an external source of vicinal diols (Figure S14 for the bidimensional microscopy images), to investigate if the already exploited polymer **1** could attract and catch soluble biomolecules along the free boronic moieties exposed on the engineered cell surface (Fig. 4). An experiment of FITC-DX catching by PDA-APBa coated silica microparticles (diatomaceous earth, Sigma Aldrich, 1 mg) has been carried out, leading to a trapping of 19% of FITC-DX from a solution containing 1 mM of the fluorescently labelled polysaccharide (Figure S16). At pH 7.8, a saturation of 72% has been achieved by loading over 60 µg of polymer. Further evidence of PDA-APBa targeting towards polysaccharides was achieved by saturation percentage curves.

These functions were obtained by using different polymer concentrations incubated for 24 h with the same amount of *Chlorella* cells and comparing the polymer absorbance recorded before and after the addition of the interacting living cells. At pH 7.8, a saturation of 72% was already reached by loading over 60 µg of the polymer

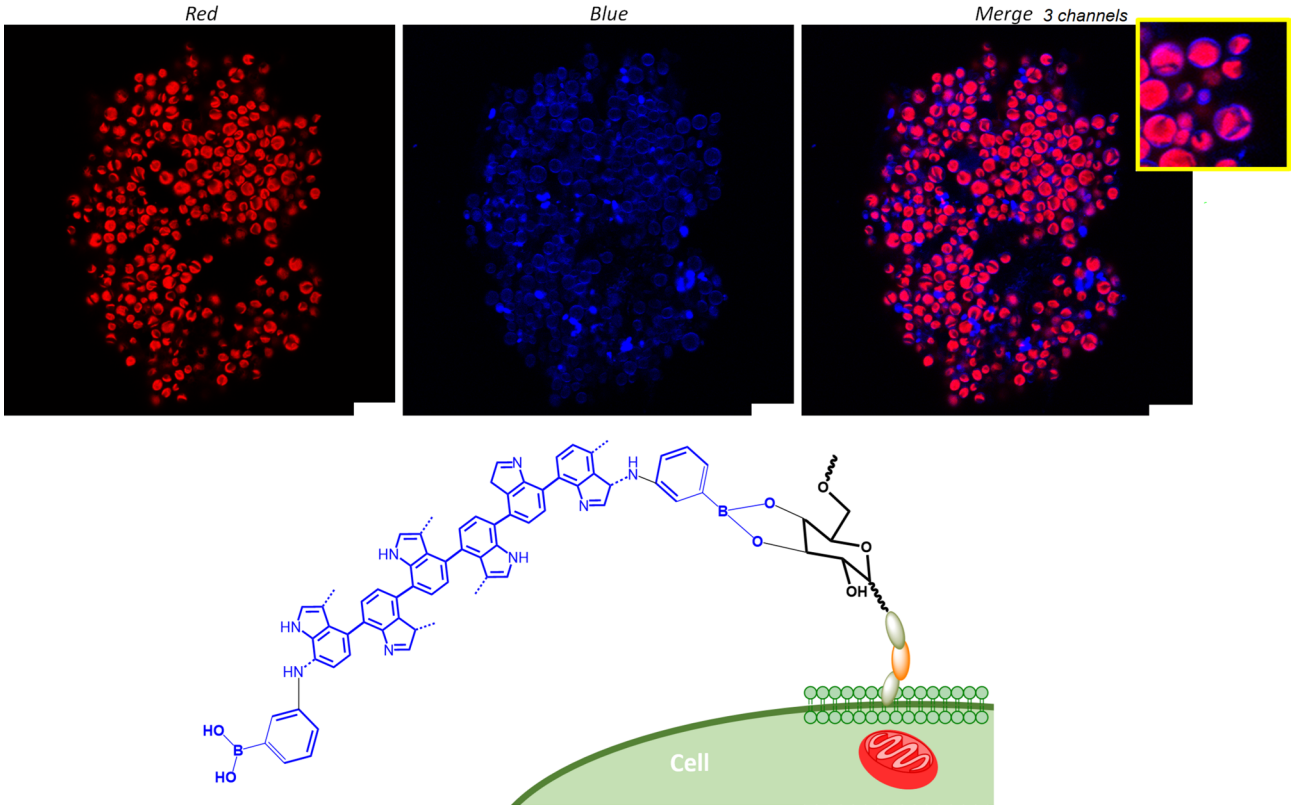

Figure 3. Confocal microscopy images of living *Chlorella* cells coated with PDA-APBa. Red and blue colors were arbitrarily assigned for chloroplast, inside cells, and PDA-APBa blue emission around cells, respectively. (Size bar 10 µm).

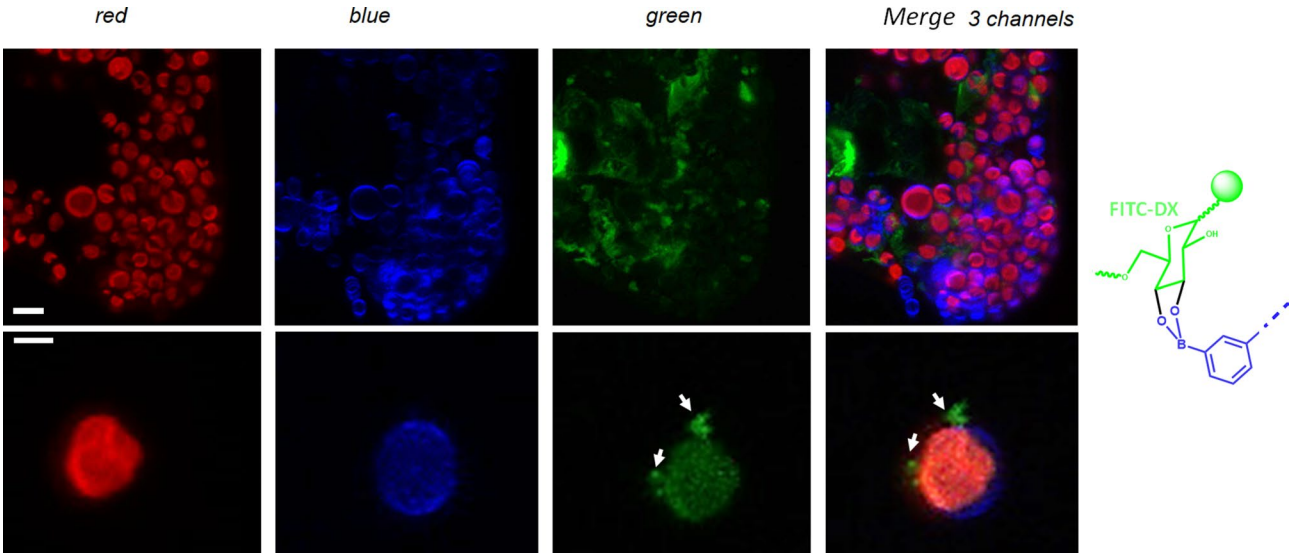

Figure 4. Confocal microscopy images of living *Chlorella* cells coated with PDA-APBa and incubated with FITC-DX. Red and blue colors were arbitrarily assigned for chloroplasts, inside cells, and PDA-APBa around cells. Green signals, present alone and in merge mode, are related to the fluorescent polysaccharide probe. (Size bar 10 µm).

(Figure S17). The same workability function defined at pH 8.5 and at pH 6.5 reported a general set of saturation below 20%. The saturation % curves have been built also for 3 other chemical species: Alizarin Red S which targets polysaccharides (Figure S18) (Gu et al., 2010), a T-BTZ-T lipid targetting moiety (Passos et al., 2021) (Figure S19) and a Cy3-NHS(Southwick et al., 1990) typically used to chemically bind to amino-termini of free Lysine of protruding membrane proteins (Figure S20).

Similar saturation % values have been obtained between PDA-APBa and Alizarin Red S (84% for ALI), conversely to the other staining agents (saturation for T-BTZ-T 65% at 7 µg, saturation for Cy3-NHS 95% at 7 µg) and this strongly suggests a common interaction of PDA-APBa and Alizarin Red S with vicinal diols of the exposed polysaccharides functionalities. In particular the rapid saturation reached by the lipophilic T-BTZ-T dye during the staining underlines the low amount of exposed lipid units, despite the abundant presence of simple sugar moieties (mainly glucose, rhamnose, mannose, xylose, galactose, arabinose and fucose)[30,31] displayed over *Chlorella* cells in glycoproteins or organized cell wall forms. Moreover, carbohydrate competition technique (displacement) has been involved to calculate the quantity of diol moiety/cell amount. As previously reported, PDA-APBa interaction with ALI leads to a fluorescence quenching, due to the production of a non fluorescent chemical specie. The displacement consists of freeing of the PDA-APBa moiety from ALI, by titrating with increasing amounts of a diol-containing chemical model (D-(+)-glucose). The delivery of the free PDA-APBa polymer causes the increase of the fluorescence of this specie, and a calibration curve can be defined, set as Fluorescence Intensity vs glucose load (Figure S21). Then, a triplicate of ALI:PDA-APBa solution has been addressed by 3 10^6 in order to displace PDA-APBa polymer from ALI, using the diol moieties present at the living cell surfaces. Then, by interpolating the calibration curve previously defined, 3 10^6 *Chlorella* cells contain 0.06 ± 0.01 mg of glucose-like moieties (with at least a diol unit/molecule). For *Thalassiosira*, *Phaeodactylum* and *Navicula* the amount of glucose-like moieties set at 0.23 ± 0.05, 0.15 ± 0.02 and 0.13 ± 0.02 mg, respectively. These values, apparently higher than those recorded for *Chlorella*, are actually taking account also of the polysaccharides not only bound over cells but also embedding the extracellular spaces. As expected, sugar moieties were not detectable for *Dunaliella* cells.

Flow cytometry has been used here both to test viability cells approaching polymer **1** and parametrizing the percentages of blue emitting polymer-coated cells and green emitting FITC-DX-binding biological systems. The cell viability analysis via flow cytometry results in 67% of living cells dispersed in the polymerization medium before coating and 57% for cells after coating treatment, as reported in histograms in Figure S22. Moreover, IC50 value for PDA-APBa was defined as 0.79 mg/mL (Figure S22). The fluorescent polymer FITC-DX has been used as an external probe biosorbed by the PDA-APBa layer over living cells. The persistence of FITC-DX was assessed during the cell growth and duplication, for several days by flow cytometry (Fig. 5). Bare cells with no polymer coating were exploited as control, while samples consisted of *Chlorella* cells incubated with PDA-APBa for 24 h. Both living samples were incubated with FITC-DX for 4 h with subsequent washing steps and then analysed. Real-time evidence of the extent of FITC-DX decoration, especially related to the presence of the organic polymer coating, was explicitly presented. The bivariate cytofluorimetric plot was obtained by recording red auto-fluorescence of chloroplasts (emission band 670 ± 15 nm) versus green FITC-DX emission (emission band 525 ± 25 nm). A significant difference is shown between control samples and polymer coated samples. Furthermore, an increase in the mean percentage of functionalized cells was observed from day 0 (90% of functionalized cells), to day 1 (99% of functionalized cells), with a decrease from 87.7 to 85.3% and to 58.8% for days 2, 3. and 6, respectively. Cytometric analysis demonstrated that cells have the ability to artificially inherit

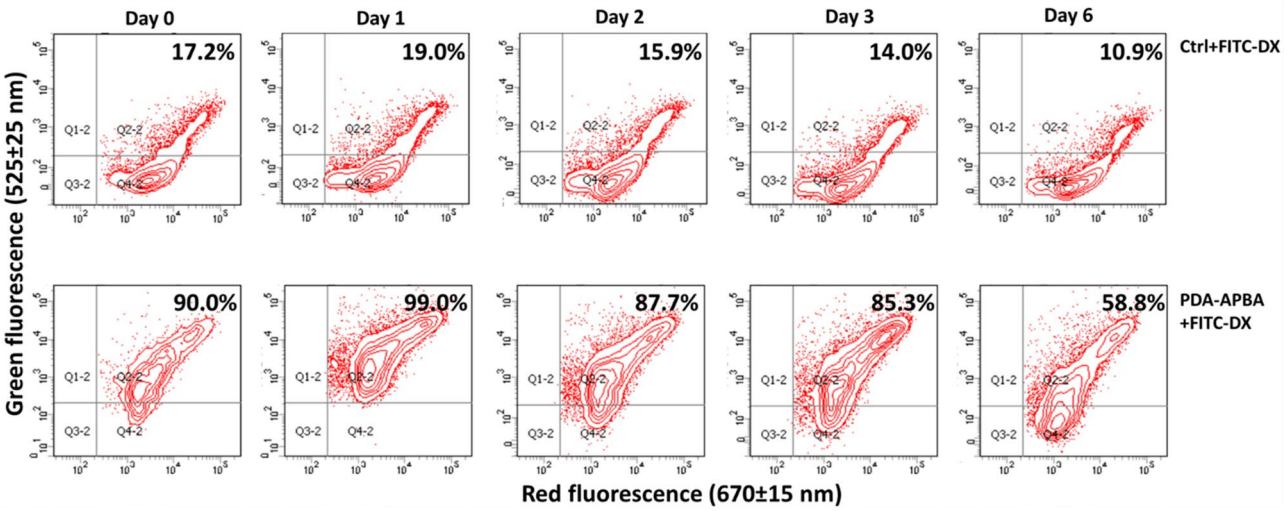

Figure 5. Artificial inheritance study of FITC-DX biosorption by flow cytometry of control cells (uncoated bare and living *Chlorella* cells) and PDA-APBa coated living *Chlorella* cells. A number of 10000 cellular events were recorded for each acquisition time, interpolating the red fluorescence values, related to chloroplast autofluorescence of living cells, versus green fluorescence values, related to the FITC emission biosorbed on the living cells.

an external decoration over time, thanks to the bridging effect offered by the PDA-APBa polymer. These results strongly suggest that the functional layer is inherited over generations. Cytometric analysis of living cells with only PDA-APBa coating was also performed, giving the following percentage positivity to the polymer coating: 35.7% for day 0, 48.2% for day 1, 62.1% for day 2, 52.4% for day 3 and 30.2% for day 6 (Figure S23). This cytometric outcome likely reflects a redistribution of the emitting polymer over the membranes along the first mitotic events (0–2 days), thus leading to a decrease of the overall quenching.

As a last evidence of the biocompatibility of polymer **1** after living cells coating, data of nutrients uptake from living microalgae biofilm, with and without polymer **1** organic coatings, have been registered here. Bare and coated samples were immersed for 6 days in their enriched semi-artificial microalgae medium, to enable living cells catch nutrients from the solutions. Then microalgae were purified, mixed with reference chemical species (see Methods), and casted/dried over plexiglass round chambers. The living biofilm were analyzed by total reflection X-ray fluorescence spectrometry (TXRF) for detecting nutrients concentration. Except for K and Mn, TXRF analysis showed an overall increase of both macro- and micronutrients concentration in coated *Chlorella* samples (Table and histograms reporting TXRF analysis results.in Fig. S24). Such an increase was particularly noteworthy for Si, Cl, Ca and Fe, and Br, less evident but present also for S, as it can be deduced from the TXRF sum-spectra comparison in Fig. 6. Among these, Ca almost doubled its concentration compared to the bare sample while Fe concentration even increased eightfold. These data suggest the possible exploitation of the organic artificial coatings to enrich living cells with useful chemical species for the molecular assembly of photosynthetic and respiratory chain, together with the likely activation and support of metabolically active enzymes present in living cells.

As final remarks, this new dopamine polymer containing phenylboronic moieties presents some specific features, starting from the possibility of easily modifying (via one-pot reaction) the monomers in aqueous buffer, under mild conditions, and the attachment of this polymer to the interface of the living cells is performed directly in water, with no harmful effects on biological systems. As a general comment, cheap and self-activating dopamine here becomes a powerful tool to produce polymeric materials carrying reactive and biologically interesting functional moieties, such as boronic species. It is so necessary to underline how the production of this supramolecular bridge occurs through a simple oxidative polymerization reaction, using oxygen as a catalyst, without consuming expensive reagents and toxic solvents, conversely to what is reported in the literature, where organic boronic-based small molecules find a peculiar place in the multidisciplinary context of functional biomaterials[32]. In details, rhodamine-based bis-boronic acids are produced via a reductive borylation with sodium boron hydride, in non-aqueous solvents, starting from diamino rhodamine dye[33]. Other cyclic boronic species proposed for targeting sugars are produced in dioxane or acetonitrile, with aliphatic amines or toxic metal catalysts[34]. Bis-boronic cross-linkers are synthesized via multistep routes, in halogenated solvents with aliphatic amines and acid activated-chlorides, with a certain ecological impact[35]. Furthermore, it is well known that PDA can be functionalized to gain the desired properties[36] exploiting Aza-Michael reactions, using small addressing molecules[37], such as thiol- or amine-terminated small molecules on pre-formed PDA, or in combination with co-polymerization of dopamine with other melanin precursors[38]. Literature proposes fully clickable polydopamine via complicated methods involving the use of dopamine bearing azide terminals to covalently couple with alkyne species[39]. Our technology, also under the perspective of the possibility to decorate polydopamine, is simple, one-pot and it yields a highly reactive self-adherent xeno-functional group. Finally, as a main intent, our outcomes underline that the PDA-APBa polymer displays boronic units over living cells,

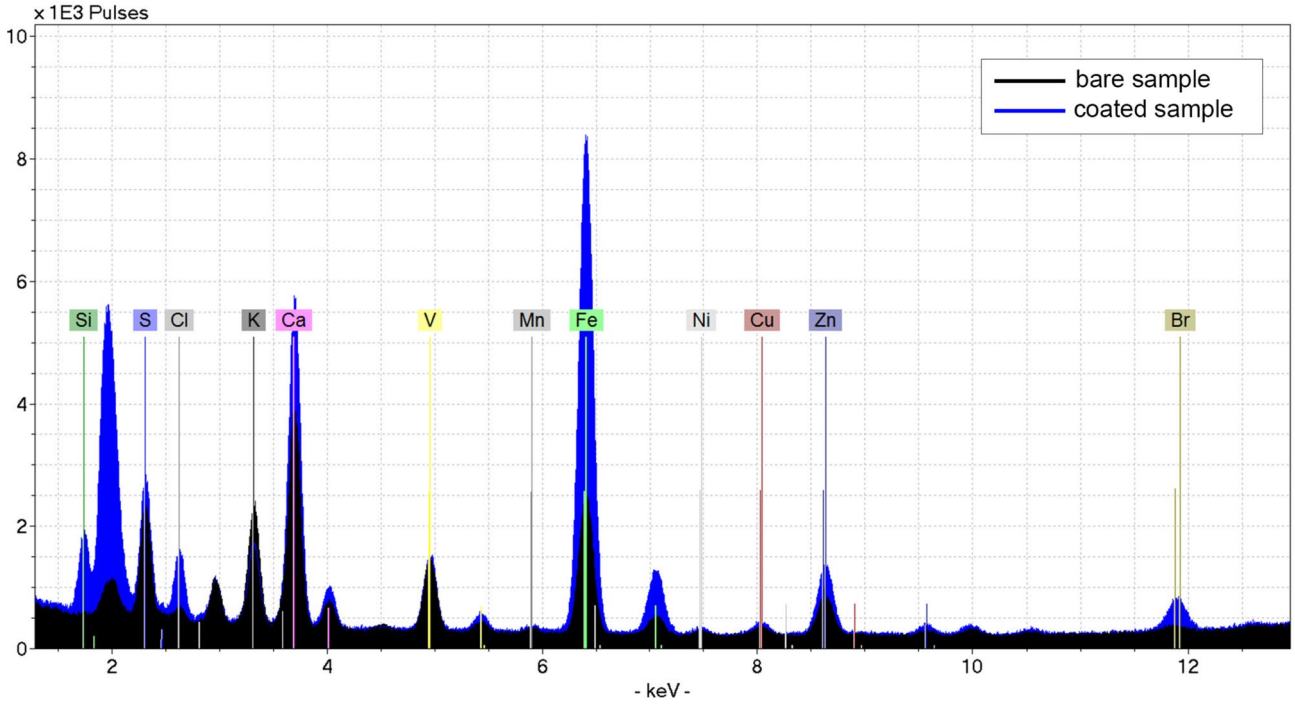

Figure 6. Comparison between the TXRF spectra of a bare sample (black) and polymer **1**-coated sample (blue). The K-lines of the elements of interest are labelled, including those of the IS (V).

which are still reactive over surfaces, and capable of interacting with specific soluble biomolecules. When the modification is applied to the cell surface, this ensures living cells an original xeno-chemical composition. This polymer technology appears ideal to tether the minimal possible amount of chemicals directly on the cell surface, with the lowest synthetic effort, aiming to realize the desired molecular recognition. Our work paves the way to produce living materials, starting from molecular to nanoscale till microscale level, consisting of engineered living cells with potentiated properties of recognition and integration of external stimuli, holding the potential for broad biological, biomedical or agritechnical applications.

Data availability

Data is provided within the manuscript or supplementary information files.

Received: 21 May 2024; Accepted: 30 July 2024
Published online: 01 August 2024

References

1. Zhou, X. Z. & Lu, K. P. The isomerase PIN1 controls numerous cancer-driving pathways and is a unique drug target. *Nat. Rev. Cancer* **16**, 463–478 (2016).
2. Laughlin, S. T. & Bertozzi, C. R. Imaging the glycome. *Proc. Natl. Acad. Sci. USA.* **106**, 12–17 (2009).
3. Lee, D. Y. *et al.* Cell surface engineering and application in cell delivery to heart diseases. *J. Biol. Eng.* **12**, 28 (2018).
4. van Swieten, P. F., Leeuwenburgh, M. A., Kessler, B. M. & Overkleeft, H. S. Bioorthogonal organic chemistry in living cells: Novel strategies for labeling biomolecules. *Org. Biomol. Chem.* **3**, 20 (2005).
5. Jeong, J. H. *et al.* Leukocyte-mimicking stem cell delivery via in situ coating of cells with a bioactive hyperbranched polyglycerol. *J. Am. Chem. Soc.* **135**, 8770–8773 (2013).
6. Shi, P. *et al.* Polyvalent display of biomolecules on live cells. *Angew. Chem. Int. Ed.* **57**, 6800–6804 (2018).
7. Buscemi, G. *et al.* Supramolecular biohybrid construct for photoconversion based on a bacterial reaction center covalently bound to cytochrome *c* by an organic light harvesting bridge. *Bioconjugate Chem.* **34**, 629–637 (2023).
8. Presti, M. L. *et al.* In vivo doped biosilica from living Thalassiosira weissflogii diatoms with a triethoxysilyl functionalized red emitting fluorophore. *MRS Adv.* **3**, 1509–1517 (2018).
9. Leone, G. *et al.* Incorporating a molecular antenna in diatom microalgae cells enhances photosynthesis. *Sci. Rep.* **11**, 5209 (2021).
10. Sletten, E. M. & Bertozzi, C. R. Bioorthogonal chemistry: Fishing for selectivity in a sea of functionality. *Angew. Chem. Int. Ed.* **48**, 6974–6998 (2009).
11. Prescher, J. A. & Bertozzi, C. R. Chemistry in living systems. *Nat. Chem. Biol.* **1**, 13–21 (2005).
12. Flemma, A. *et al.* Chemically decorated microalgae for environmental application. in *2022 IEEE International Workshop on Metrology for the Sea; Learning to Measure Sea Health Parameters (MetroSea)* 101–105 (IEEE, Milazzo, Italy, 2022). https://doi.org/10.1109/MetroSea55331.2022.9950904.
13. Buscemi, G. *et al.* Bio-inspired redox-adhesive polydopamine matrix for intact bacteria biohybrid photoanodes. *ACS Appl. Mater. Interfaces* **14**, 26631–26641 (2022).
14. Buscemi, G. *et al.* Polydopamine/ethylenediamine nanoparticles embedding a photosynthetic bacterial reaction center for efficient photocurrent generation. *Adv. Sustainable Syst.* **5**, 2000303 (2021).
15. Cicco, S. R. *et al.* Improving the in vitro removal of indoxyl sulfate and p-Cresyl sulfate by coating diatomaceous earth (DE) and poly-vinyl-PYRROLIDONE-co-styrene (PVP-co-S) with polydopamine. *Toxins* **14**, 864 (2022).

16. Aresta, A., Cicco, S. R., Vona, D., Farinola, G. M. & Zambonin, C. Mussel inspired polydopamine as silica fibers coating for solid-phase microextraction. *Separations* **9**, 194 (2022).
17. Cai, S., Cheng, Y., Qiu, C., Liu, G. & Chu, C. The versatile applications of polydopamine in regenerative medicine: Progress and challenges. *Smart Mater. Med.* **4**, 294–312 (2023).
18. Ambrico, M. *et al.* Engineering polydopamine films with tailored behaviour for next-generation eumelanin-related hybrid devices. *J. Mater. Chem. C* **1**, 1018–1028 (2013).
19. Allegretta, I. *et al.* Determination of As concentration in earthworm coelomic fluid extracts by total-reflection X-ray fluorescence spectrometry. *Spectrochimica Acta Part B Atomic Spectroscopy* **130**, 21–25 (2017).
20. Liu, X. *et al.* Amine-triggered dopamine polymerization: From aqueous solution to organic solvents. *Macromol. Rapid Commun.* **39**, 1800160 (2018).
21. Vona, D. *et al.* Boronic acid moieties stabilize adhesion of microalgal biofilms on glassy substrates: A chemical tool for environmental applications. *ChemBioChem* https://doi.org/10.1002/cbic.202300284 (2023).
22. Kurt, M., Raci Sertbakan, T., Özduran, M. & Karabacak, M. Infrared and Raman spectrum, molecular structure and theoretical calculation of 3,4-dichlorophenylboronic acid. *J. Molecular Struct.* **921**, 178–187 (2009).
23. Hadjiivanov, K. I. *et al.* Power of infrared and Raman spectroscopies to characterize metal-organic frameworks and investigate Their interaction with guest molecules. *Chem. Rev.* **121**, 1286–1424 (2021).
24. Kajisa, T., Li, W. & Michinobu, T. Catecholamine detection using a functionalized Poly(L -dopa)-coated gate field-effect transistor. *ACS Omega* **3**, 6719–6727 (2018).
25. Springsteen, G. & Wang, B. A detailed examination of boronic acid–diol complexation. *Tetrahedron* **58**, 5291–5300 (2002).
26. Mócsai, R. *et al.* N-glycans of the microalga Chlorella vulgaris are of the oligomannosidic type but highly methylated. *Sci. Rep.* **9**, 331 (2019).
27. Wang, X., Xia, N. & Liu, L. Boronic acid-based approach for separation and immobilization of glycoproteins and its application in sensing. *IJMS* **14**, 20890–20912 (2013).
28. Liu, L. *et al.* A versatile dynamic mussel-inspired biointerface: From specific cell behavior modulation to selective cell isolation. *Angew. Chem. Int. Ed.* **57**, 7878–7882 (2018).
29. Narkar, A. R., Barker, B., Clisch, M., Jiang, J. & Lee, B. P. pH responsive and oxidation resistant wet adhesive based on reversible catechol-boronate complexation. *Chem. Mater.* **28**, 5432–5439 (2016).
30. Takeda, H. Sugar composition of the cell wall and the taxonomy of *chlorella* (CHLOROPHYCEAE)[1]. *J. Phycol.* **27**, 224–232 (1991).
31. El-Naggar, N.E.-A., Hussein, M. H., Shaaban-Dessuuki, S. A. & Dalal, S. R. Production, extraction and characterization of Chlorella vulgaris soluble polysaccharides and their applications in AgNPs biosynthesis and biostimulation of plant growth. *Sci. Rep.* **10**, 3011 (2020).
32. Akgun, B. & Hall, D. G. Boronic acids as bioorthogonal probes for site-selective labeling of proteins. *Angew. Chem. Int. Ed.* **57**, 13028–13044 (2018).
33. Kim, K. K. *et al.* Postcolumn HPLC detection of mono- and oligosaccharides with a chemosensor. *Org. Lett.* **5**, 5007–5010 (2003).
34. Andersen, K. A., Smith, T. P., Lomax, J. E. & Raines, R. T. Boronic acid for the traceless delivery of proteins into cells. *ACS Chem. Biol.* **11**, 319–323 (2016).
35. Shin, S. B. Y., Almeida, R. D., Gerona-Navarro, G., Bracken, C. & Jaffrey, S. R. Assembling ligands in situ using bioorthogonal boronate ester synthesis. *Chem. Biol.* **17**, 1171–1176 (2010).
36. Lee, H., Dellatore, S. M., Miller, W. M. & Messersmith, P. B. Mussel-inspired surface chemistry for multifunctional coatings. *Science* **318**, 426–430 (2007).
37. Liu, C.-Y. & Huang, C.-J. Functionalization of polydopamine via the Aza-michael reaction for antimicrobial interfaces. *Langmuir* **32**, 5019–5028 (2016).
38. Wang, G., Huang, X. & Jiang, P. Mussel-inspired fluoro-polydopamine functionalization of titanium dioxide nanowires for polymer nanocomposites with significantly enhanced energy storage capability. *Sci. Rep.* **7**, 43071 (2017).
39. Bisht, H., Jeong, J., Hong, Y., Park, S. & Hong, D. Development of Universal and clickable film by mimicking melanogenesis: On-demand oxidation of tyrosine-based azido derivative by tyrosinase. *Macromol. Rapid Commun.* **43**, 2200089 (2022).

Acknowledgements

The student Matteo Cavaliere is acknowledged for this paper. This work regarded the Agritech National Research Center funding from the European Union Next-Generation EU (PIANO NAZIONALE DI RIPRESA E RESILIENZA (PNRR)–MISSIONE 4 COMPONENTE 2, INVESTIMENTO 1.4–D.D. 1032 17/06/2022, CN00000022). This work also refers to Dipartimenti di Eccellenza-progetto MAR.V.E.L. (MARginal areas: Valorization of Ecosystem resources for fair and sustainable Livelihood, ICT-2018-20) and H2020-MSCA-ITN-2019 project860125-BEEP (Bioinspired and bionic materials for enhanced photosynthesis).

Author contributions

D.V. and S.R.C. for conceptualization of chemical work, writing and proof reading; C.V.G. and A.D. for the cell cultures and sterile conditions; G.R. and R.L. for living cells decoration and preliminary characterizations; M.M.G. for Raman Spectroscopy; E.A. confocal microscopy and flow cytometry analysis; C.P. and R.T. for TXRF analysis; E.A., P.C. and G.M.F. for conceptualization, writing, proof reading and design of the biological and chemical experiments.

Competing interests

The authors declare no competing interests.

Additional information

Supplementary Information The online version contains supplementary material available at https://doi.org/10.1038/s41598-024-68932-4.

Correspondence and requests for materials should be addressed to P.C.

Supplementary Information

A melanin-like polymer bearing phenylboronic units as a suitable bioplatform for living cell display technology

Danilo Vona†[a], Stefania Roberta Cicco†[b], Cesar Vicente-Garcia[c], Alessandro Digregorio[c], Giorgio Rizzo [c], Rossella Labarile[d], Maria Michela Giangregorio[e], Carlo Porfido[a], Roberto Terzano[a], Emiliano Altamura[c]*, Pietro Cotugno[c]*, Gianluca Maria Farinola[c]

Affiliations:

a. Dipartimento di Scienze del Suolo, della Pianta e degli Alimenti (Di.S.S.P.A.), Università Degli Studi di Bari "Aldo Moro", Via G. Amendola 165/A, 70126 Bari, Italy

b. Consiglio Nazionale delle Ricerche, CNR-ICCOM, Via E. Orabona 4, 70126 Bari, Italy

c. Dipartimento di Chimica, Università Degli Studi di Bari "Aldo Moro", Via E. Orabona 4, 70126 Bari, Italy

d. Consiglio Nazionale delle Ricerche, IPCF-CNR, Via E. Orabona 4, 70126 Bari, Italy

e. Institute of Nanotechnology, CNR-NANOTEC, Via Orabona 4, 70126 Bari, Italy

† These Authors equally contributed as first names

* Corresponding authors

† These Authors equally contributed as first names

*Corresponding authors

emiliano.altamura@uniba.it; pietro.cotugno@uniba.it

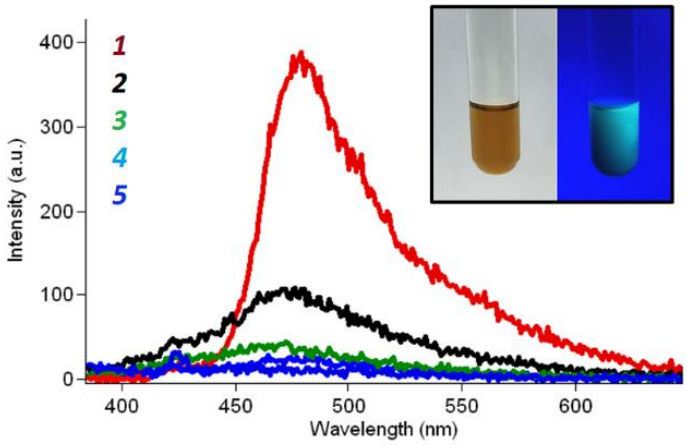

Figure S1|Fluorescence spectra recorded for polymers obtained from dopamine and different aminoarenes polymerization.

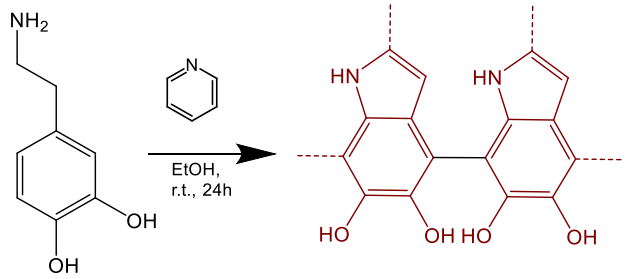

Figure S2|Scheme of dopamine polymerization in presence of pyridine as base catalyst.

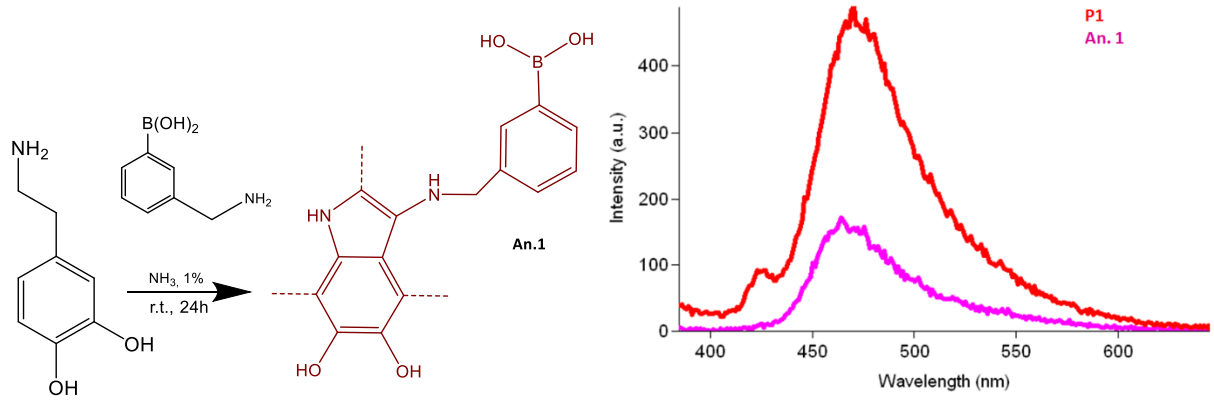

Figure S3| Scheme of dopamine polymerization with 3-aminomethylphenylboronic acid and related fluorescence spectrum compared with PDA-APBa.

Figure S4 shows Raman spectra of PDA films drop casted on silicon_before (PDA) and after doping with 3-aminophenylboronic acid (PDA-APBa) compared with the Raman spectrum of the reference 3-aminophenylboronic acid (APBa), in three different ranges, (a) 1000-1450 cm^{-1}, (b) 1000-2000 cm^{-1} and 2700-3700 cm^{-1}. Spectra of all

the samples in the range 1000-2000 cm^{-1} (figure S4(b)) are dominated by very intense bands due to C-C, C-N and CO stretching, and the band due to O-B stretching at around 1450 cm^{-1} of the APBa precursor cannot be discriminated in PDA-APBa because it overlaps to C-C stretching band of PDA. Zooming the measurement range and focalizing between 1000-1450 cm^{-1}, as shown in Figure S4a, changes in the Raman spectra can be emphasized. Specifically, after doping with 3-aminophenylboronic acid (red lines), Raman spectra of pure PDA show the presence of additional peaks, indicated by red asterisks, due to the formation of bonds between B,C and O atoms. Finally Figure S4c shows bands due to CH and OH bonds for pure PDA, PDA-APBa and APBa precursor without no significant differences.

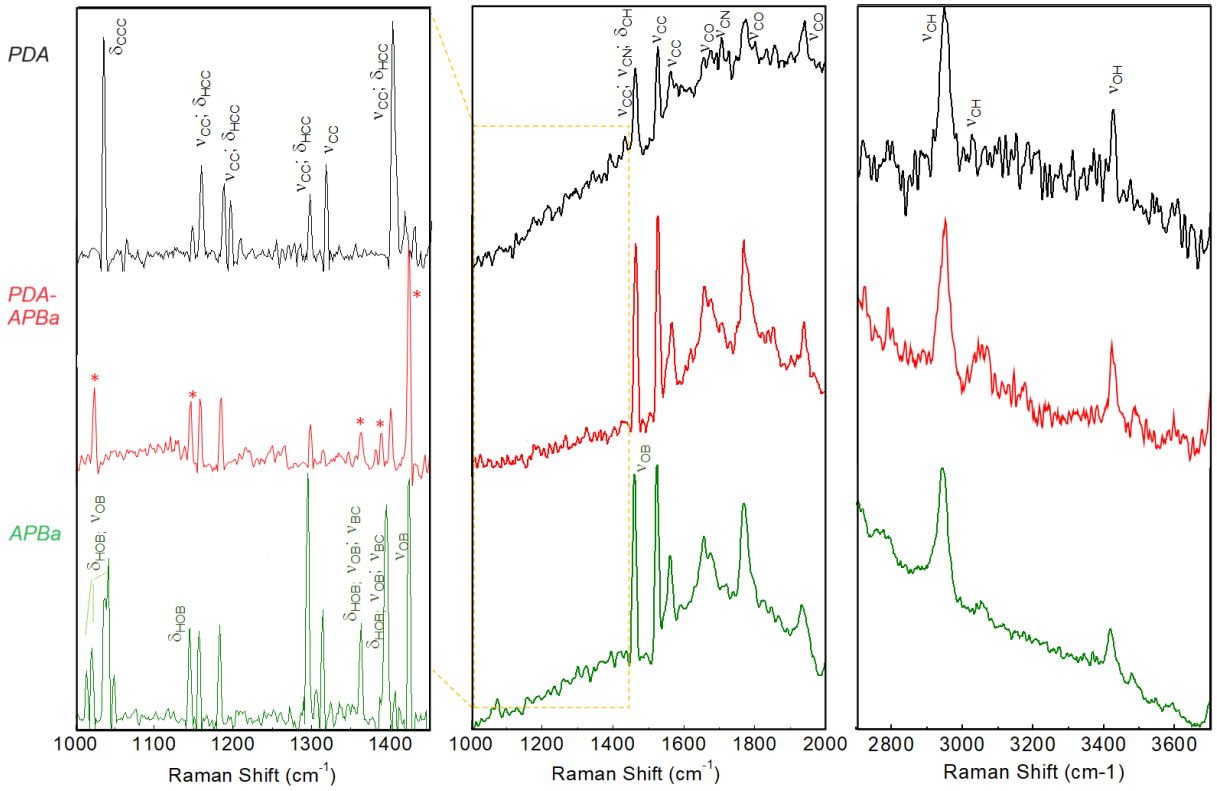

Figure S4| Raman spectra of PDA films on silicon before (pure; black lines) and after doping by 3-aminophenylboronic acid (B-doped; red lines) compared with the Raman spectrum of the reference 3-aminophenylboronic acid (B-precursor; green lines) in two wide ranges (b) 1000-2000 cm^{-1} and 2700-3700 cm^{-1} and in a zoomed one (a) 1000-1450cm^{-1}. OH/CO/CC/CN/CH and B-C/B-O modes are indicated in black and green, respectively, while red asterisks in the Raman spectra of B-doped PDA films indicate the formation of B-C/B-O modes not present in pure PDA. Raman vibrations, $\wp$ (torsion), ™ (bending), ⦚ (stretching) and ⟩(rocking) are also specified.

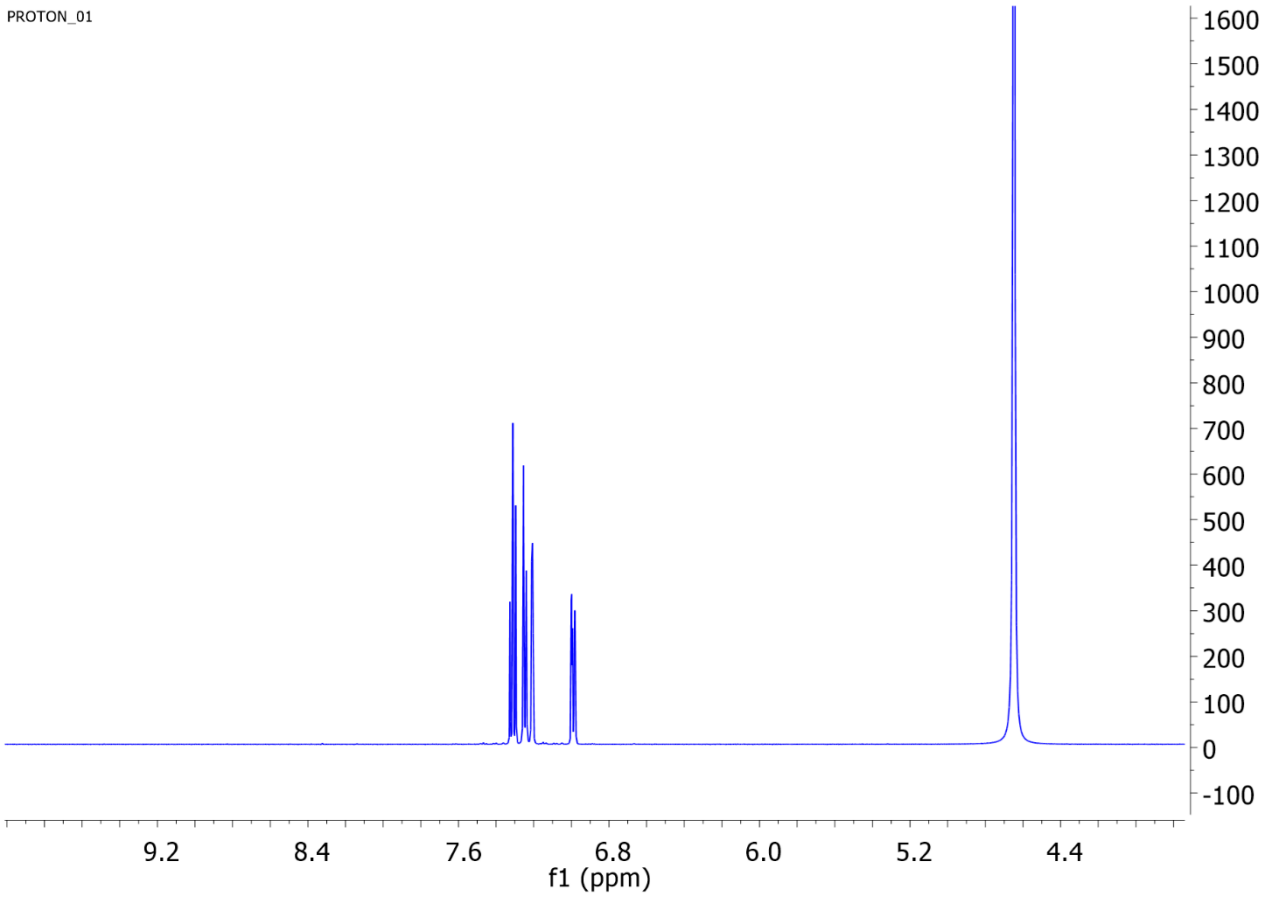
PROTON_01
1600
1500
1400
1300
1200
1100
1000
900
800
700
600
500
400
300
200
100
0
-100
9.2
8.4
7.6
6.8
6.0
5.2
4.4
f1 (ppm)

APBa

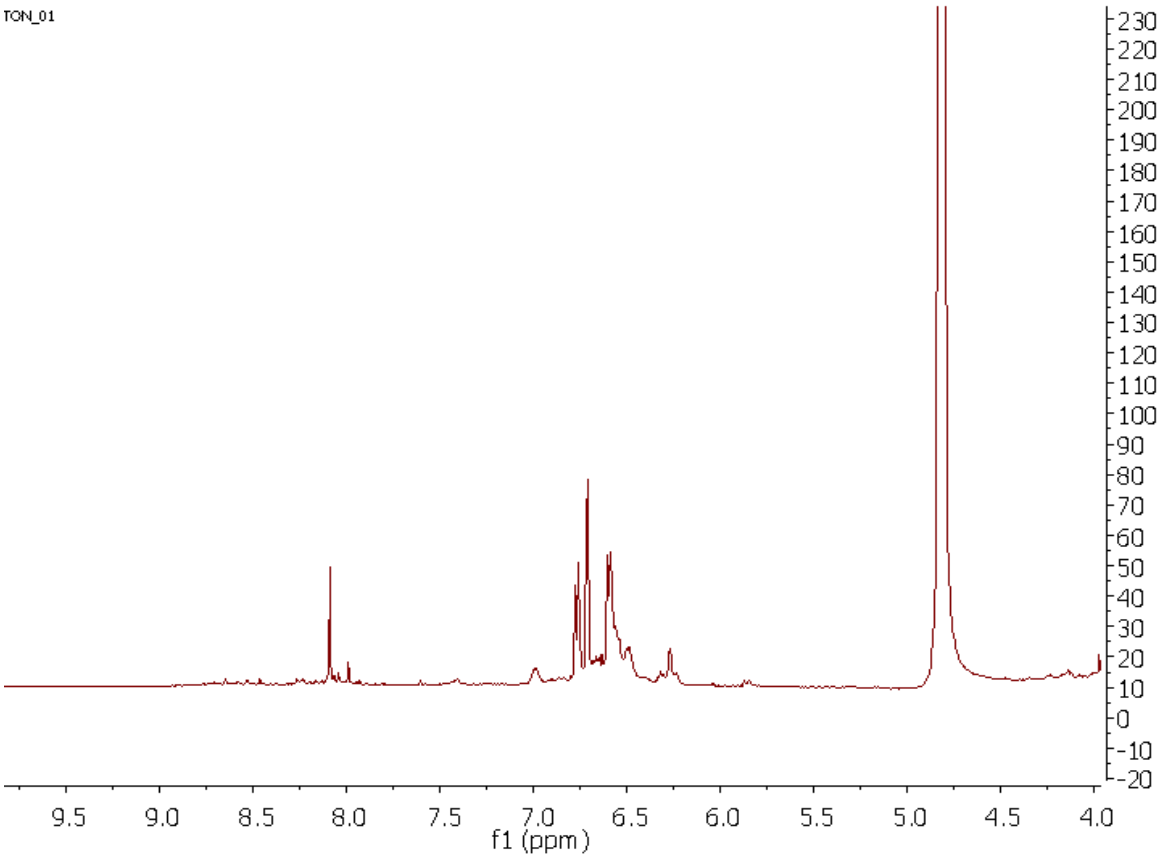
TON_01
230
220
210
200
190
180
170
160
150
140
130
120
110
100
90
80
70
60
50
40
30
20
10
0
-10
-20
9.5
9.0
8.5
8.0
7.5
7.0
6.5
6.0
5.5
5.0
4.5
4.0
f1 (ppm)

PDA-APBa

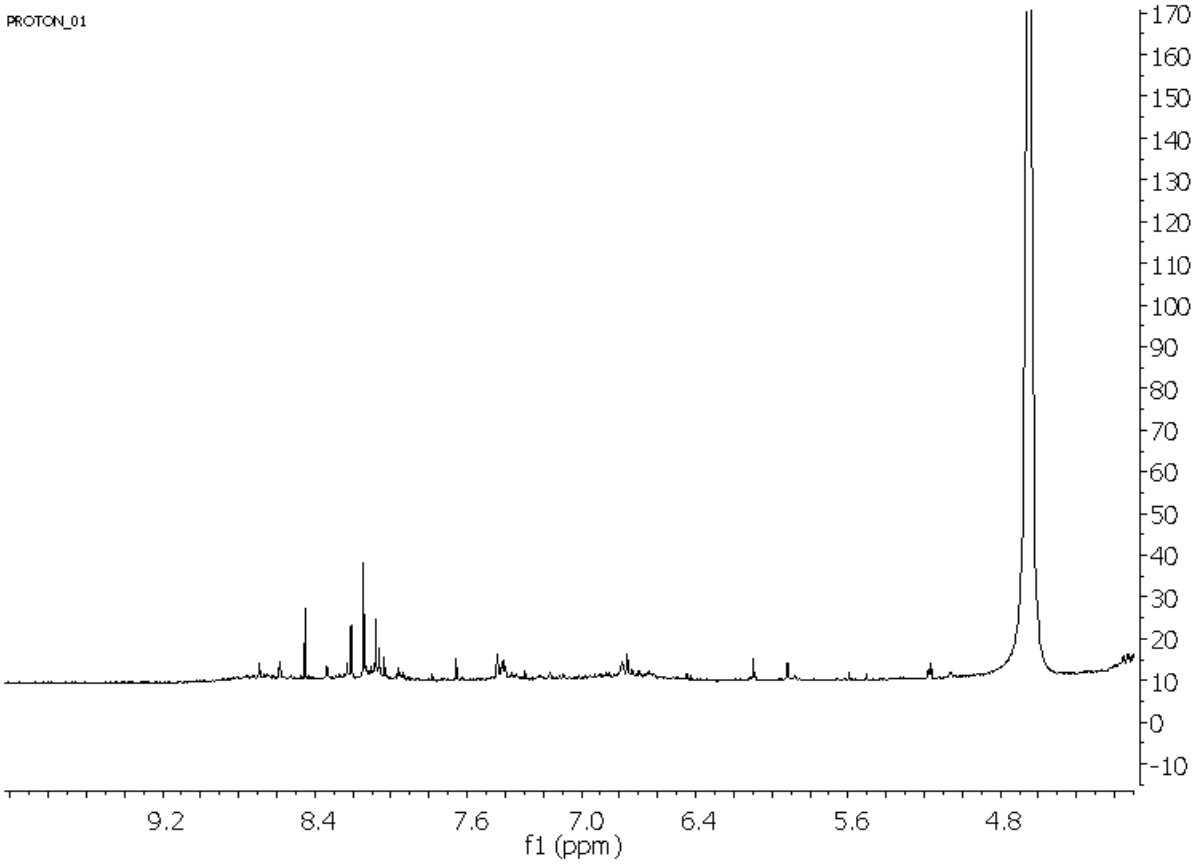
PROTON_01
170
160
150
140
130
120
110
100
90
80
70
60
50
40
30
20
10
0
-10
9.2
8.4
7.6
7.0
6.4
5.6
4.8
f1 (ppm)

PDA

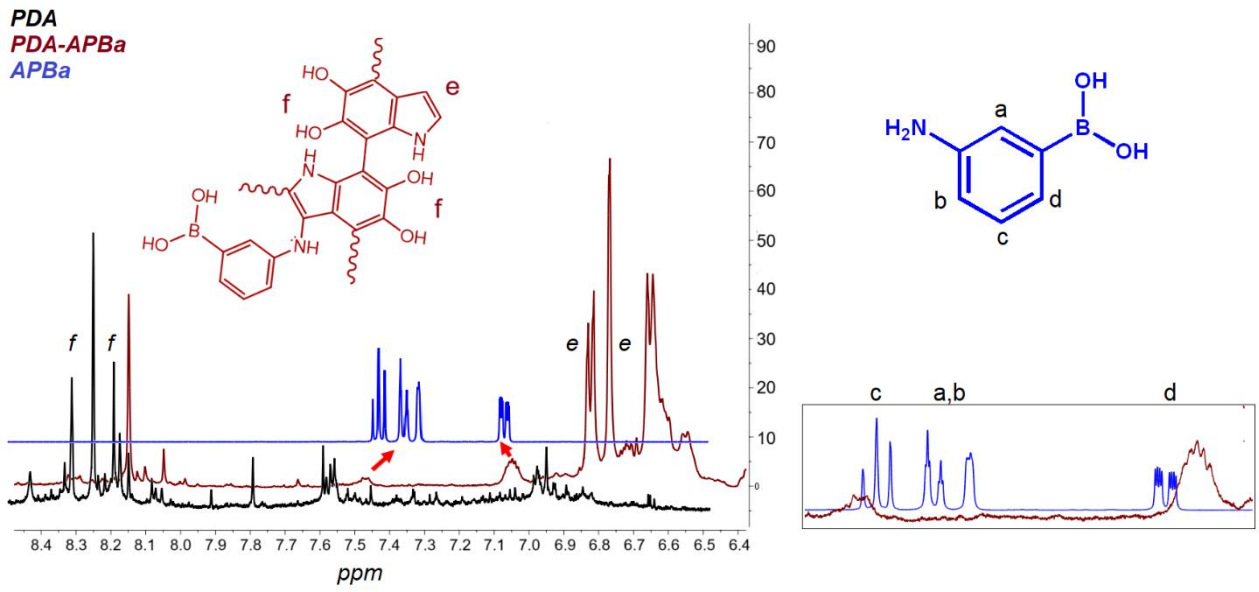
PDA
PDA-APBa
APBa
HO
f
HO
e
N
H
N
H
OH
f
OH
HO
B
OH
NH
OH
f
f
e
e
90
80
70
60
50
40
30
20
10
0
8.4 8.3 8.2 8.1 8.0 7.9 7.8 7.7 7.6 7.5 7.4 7.3 7.2 7.1 7.0 6.9 6.8 6.7 6.6 6.5 6.4
ppm
OH
a
H2N
B
OH
b
d
c
c
a,b
d

Figure S5|[1]H-NMR of APBa, PDA-APBa and PDA with related focus and merge.

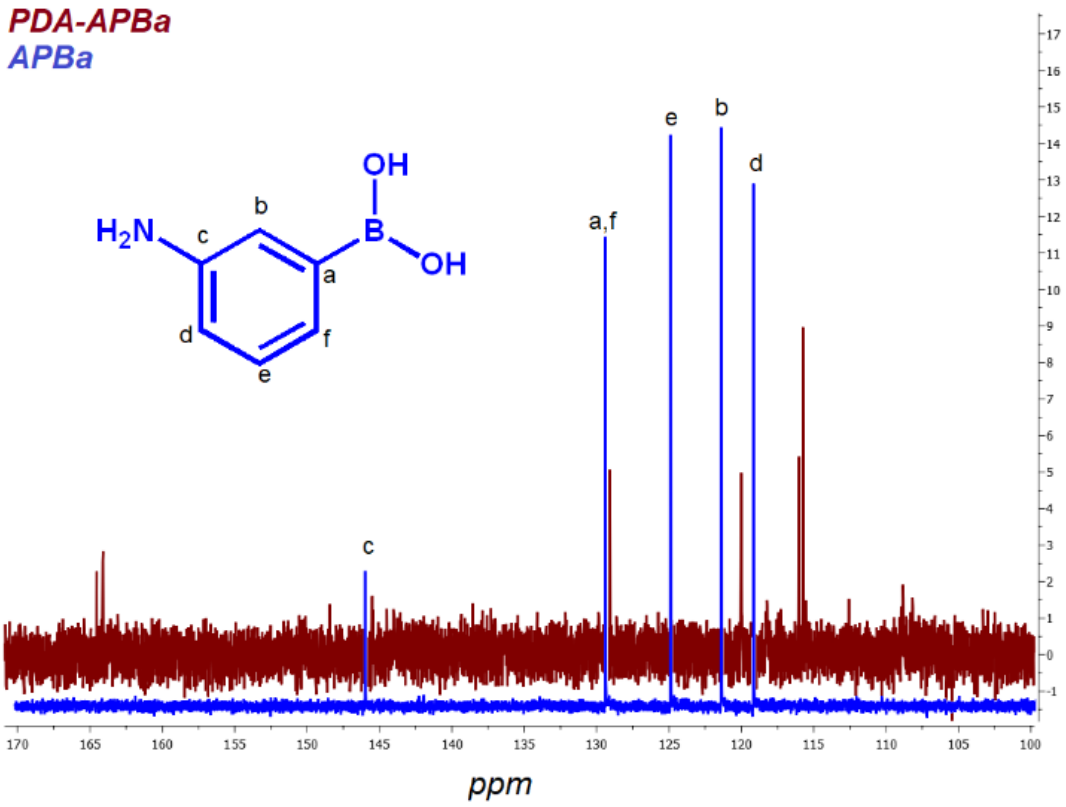

Figure S6| [13]C-NMR of PDA-APBa and APBa.

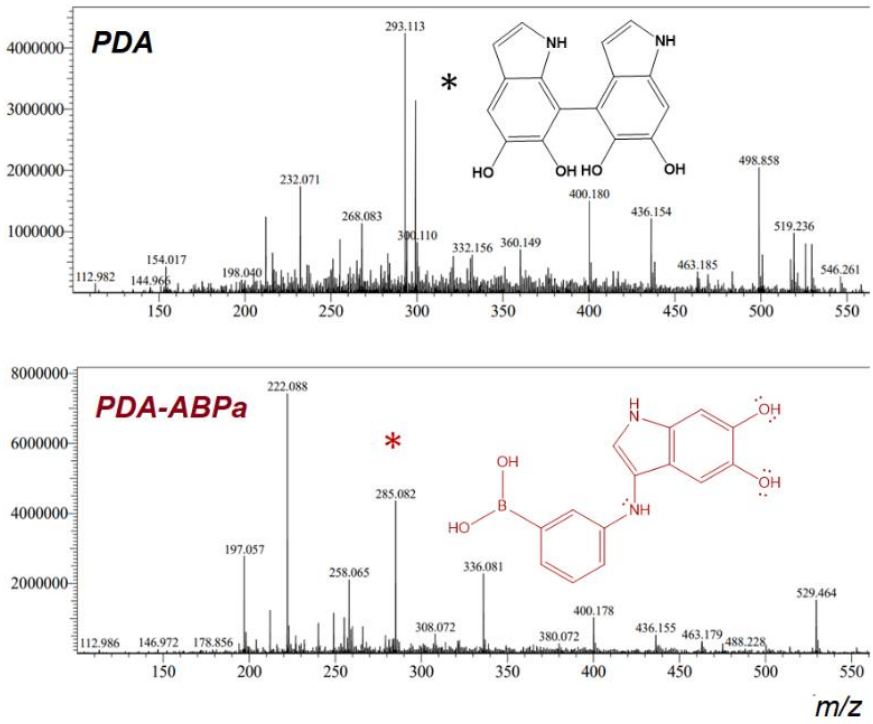

Figure S7| LC-MS comparison of washing solutions from polymerization of dopamine (PDA) and dopamine+APBa (PDA-APBa).

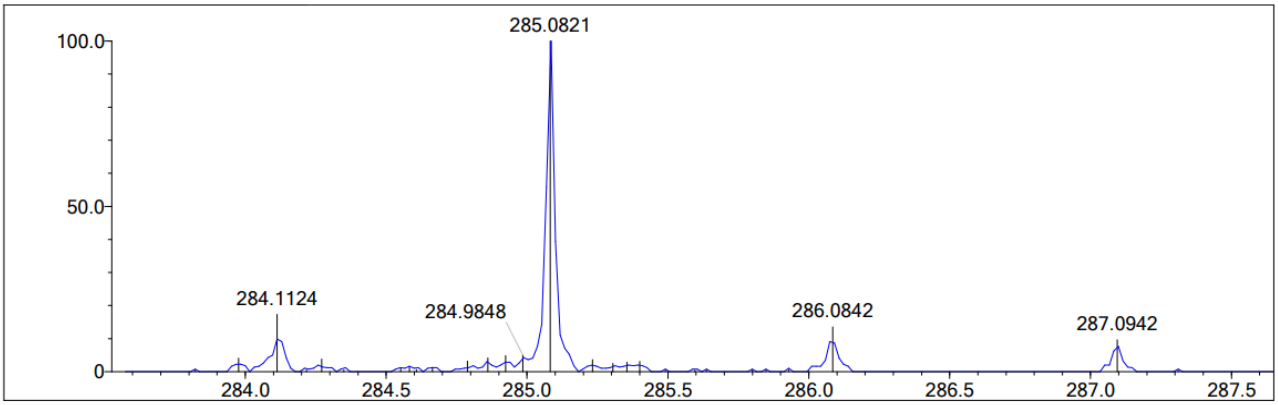

Figure S8|MS fragmentation pattern of dopamine-APBa dimer.

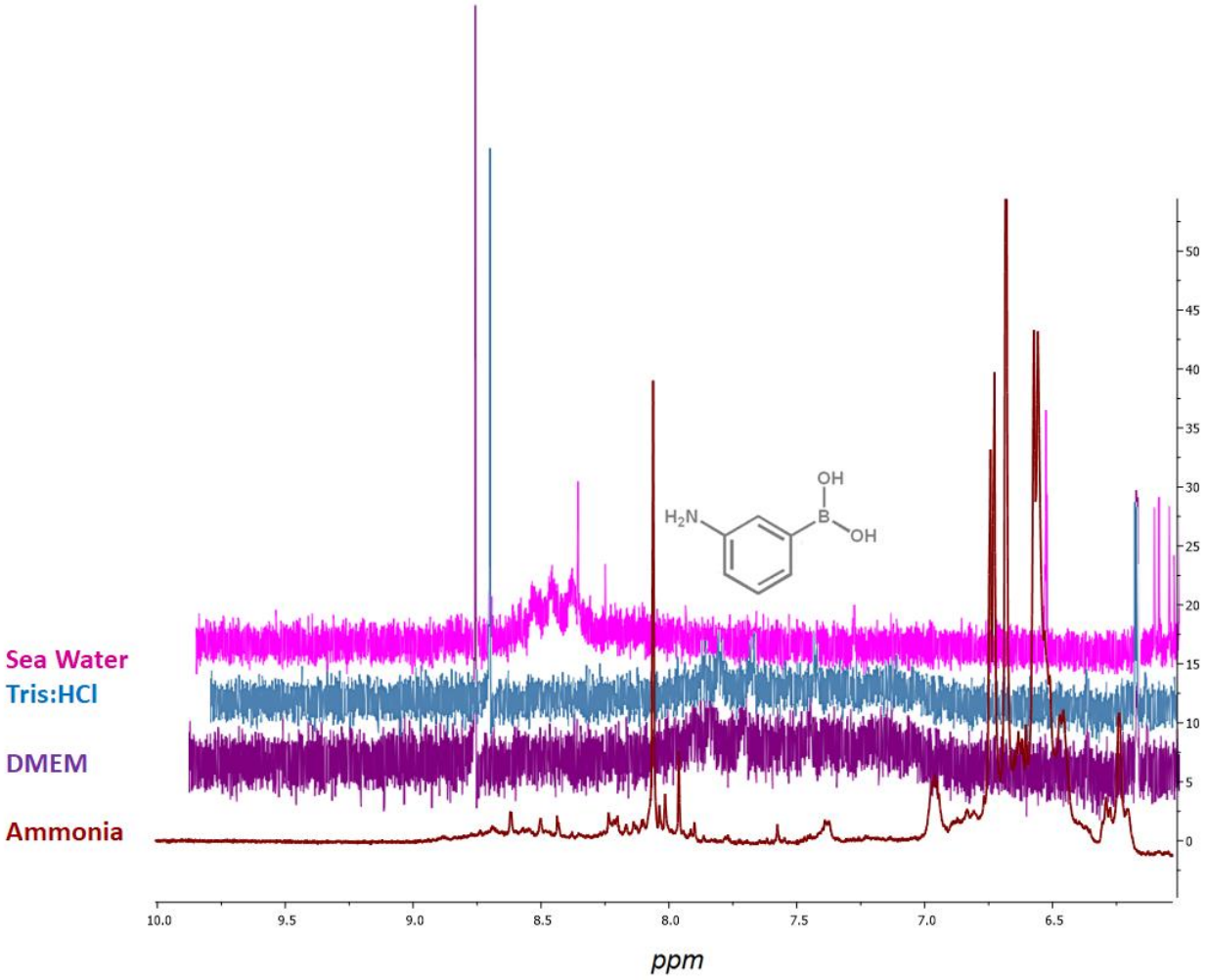

Figure S9| ^{1}H-NMR of PDA-APBa obtained in different biocompatible media (D_2O as suitable solvent for NMR experiment).

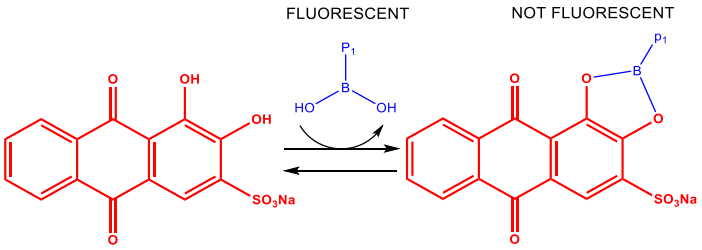

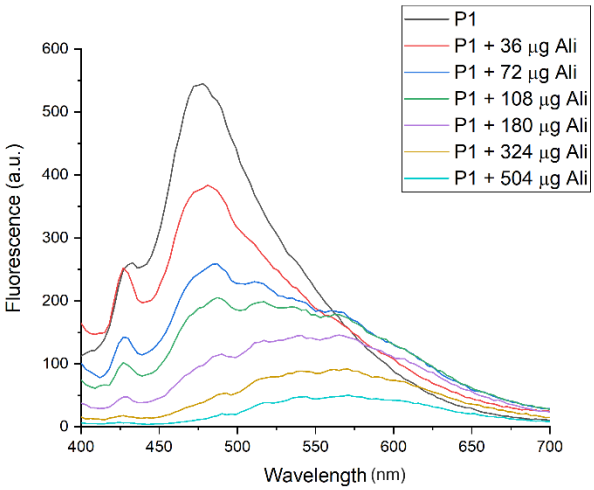

Figure S10| Kinetics of quenching of PDA-APBa emission (exc.: 385 nm; em.: 475 nm) to reach the saturation of boronic functionalities.

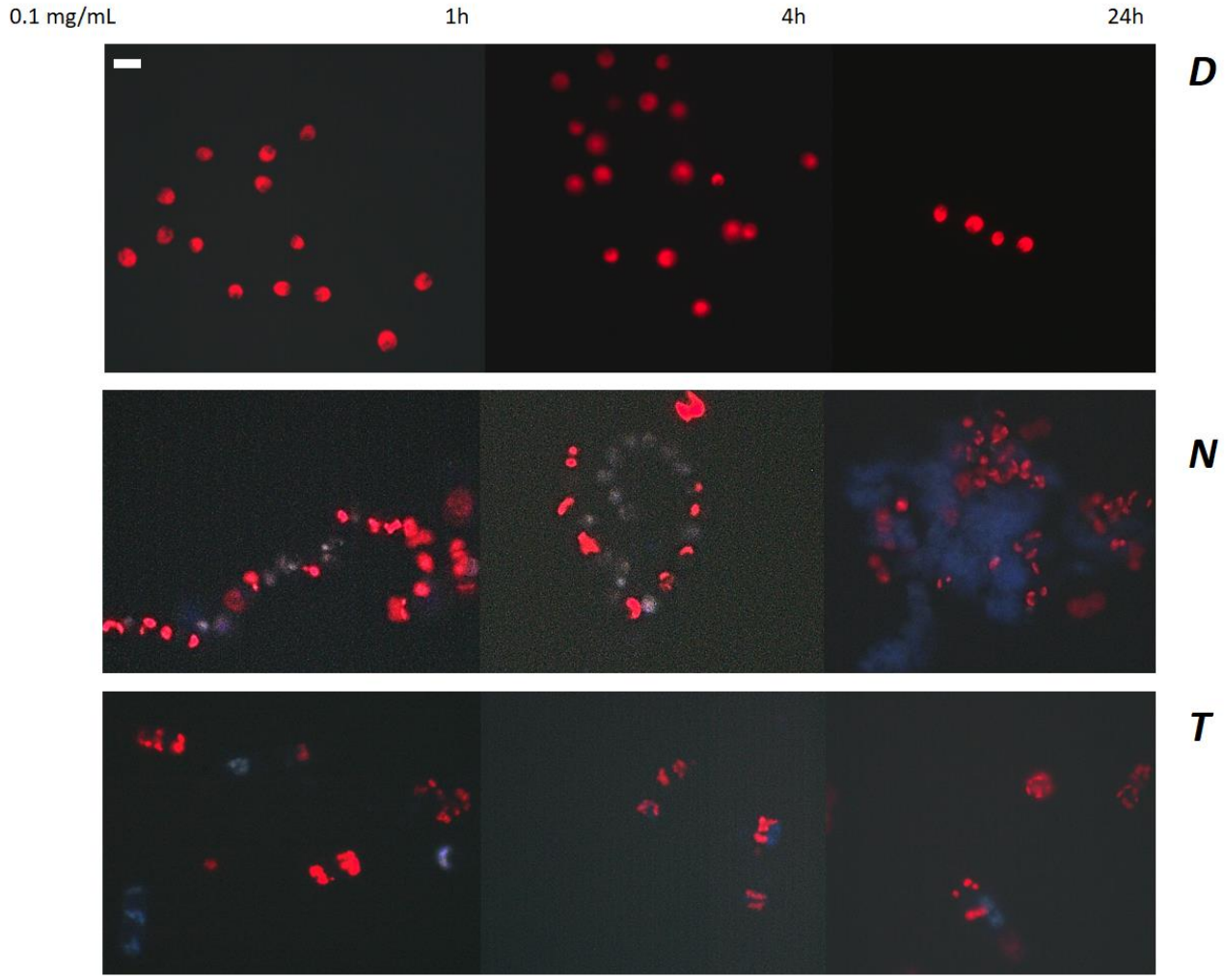

Figure S11|Bidimensional fluorescence microscopy images, in merge mode, of different microalgae stained with PDA-APBa (*Dunaliella*, *Navicula*, *Thalassiosira*).

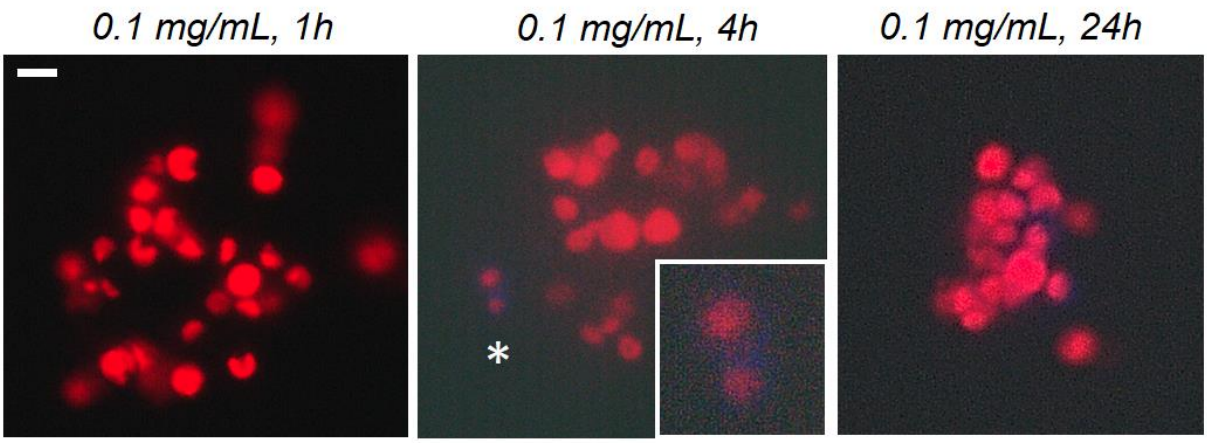

Figure S12| Bidimensional fluorescence microscopy images, in merge mode, of *Chlorella* microalgae stained with PDA-APBa using different incubation times.

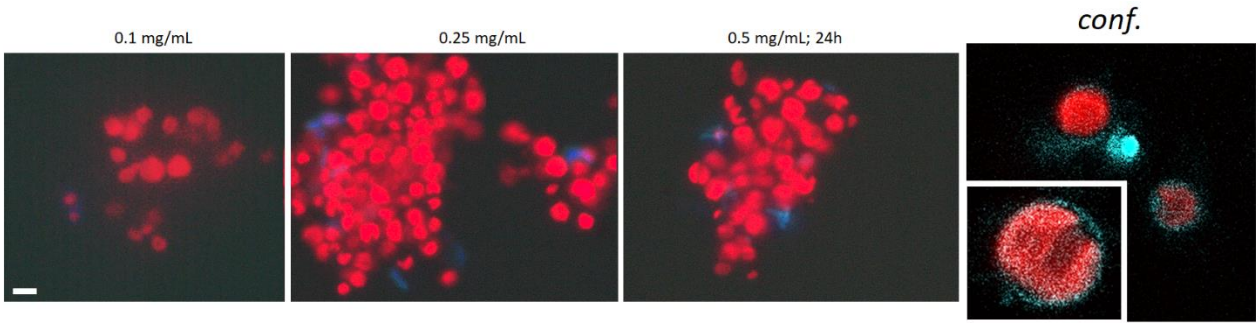

Figure S13| Bidimensional fluorescence microscopy images, in merge mode, of *Chlorella* microalgae stained with PDA-APBa for different polymer concentration, after 24 hours of incubation; the focus is related to the confocal imaging.

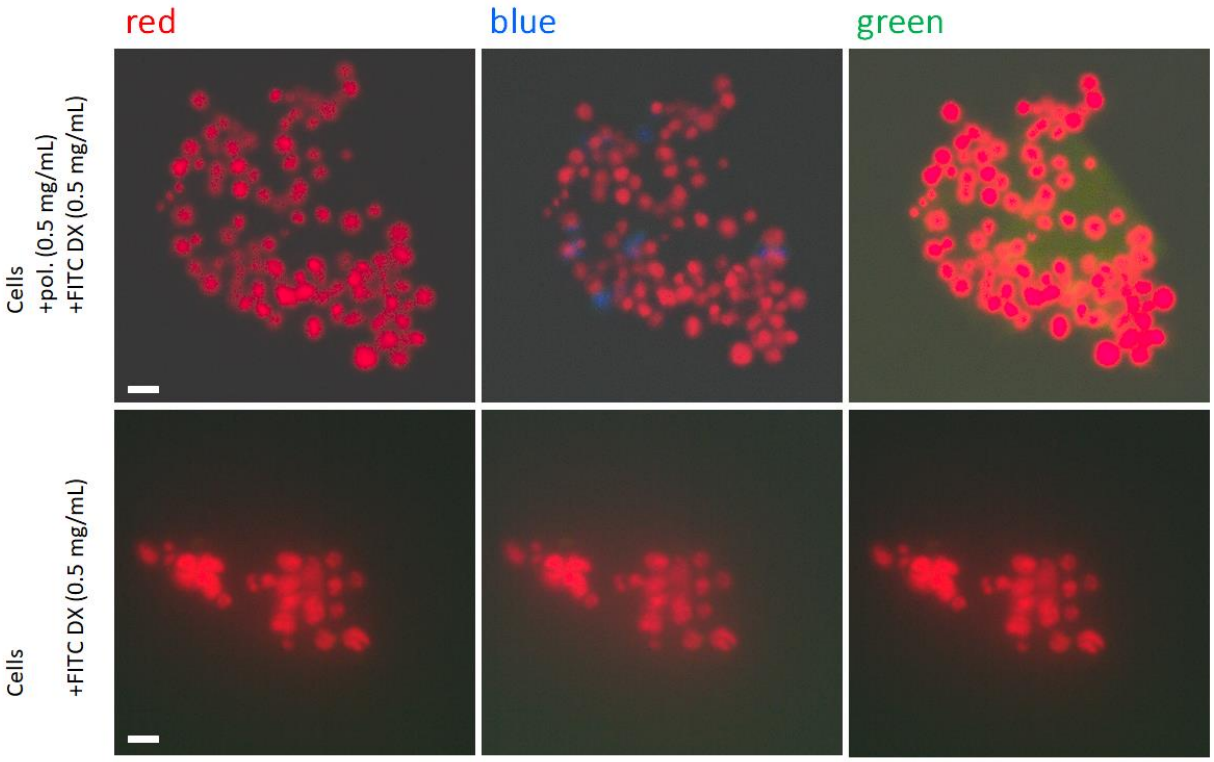

Figure S14| Bidimensional fluorescence microscopy images, in merge mode, of *Chlorella* microalgae stained with PDA-APBa and incubated with FITC DX, in comparison with control cells.

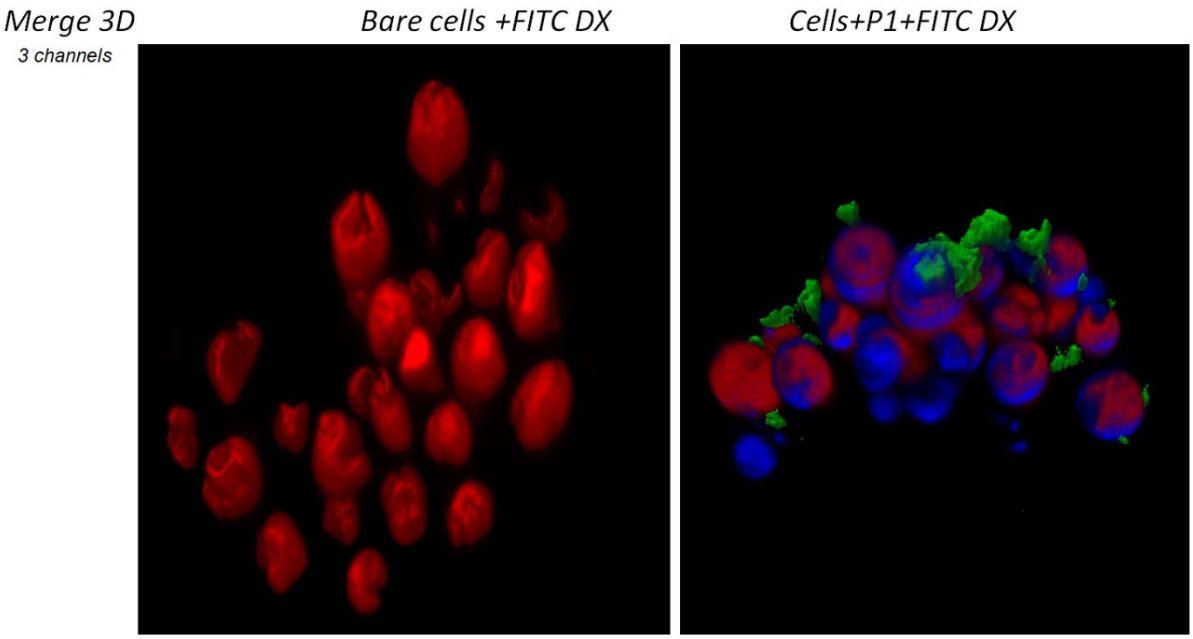

Figure S15| 3D reconstruction of *Chlorella* microalgae stained with PDA-APBa and incubated with FITC DX.

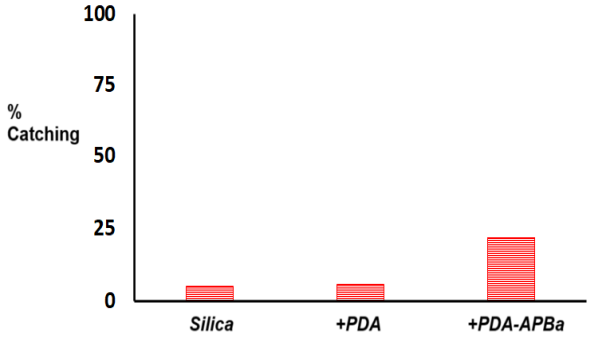

Figure S16| Histograms related to the catching evaluation of silica microparticles before (silica), after PDA-coating (+PDA) and after PDA-APBa-coating (+PDA-APBa) towards 1 mM FITC DX in sea water.

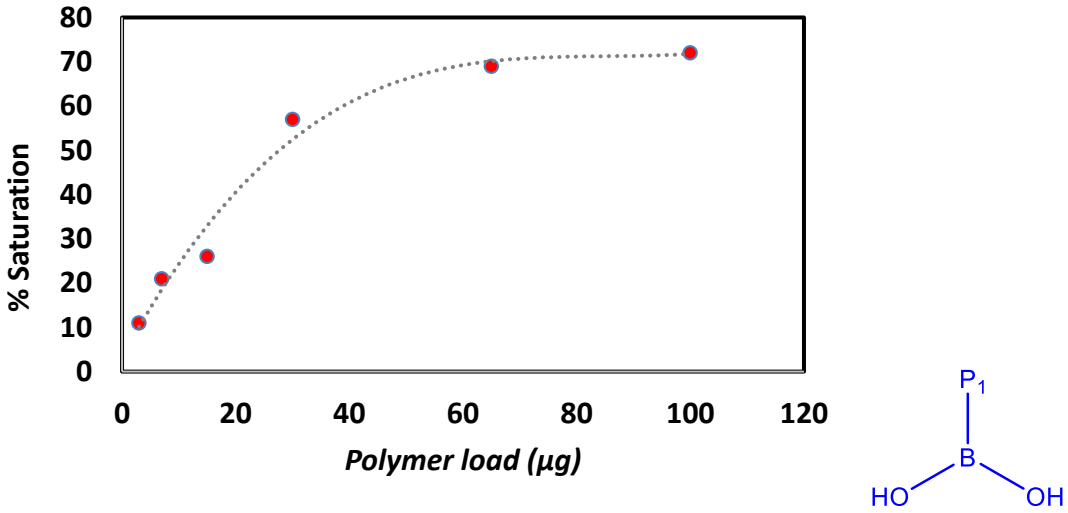

Figure S17| Saturation % curve defined using different loads of PDA-APBa towards the same amount of living Chlorella cells. Absorbances have been evaluated at 419 nm after 24 hours of incubation and investigating the supernatants with and without living cells.

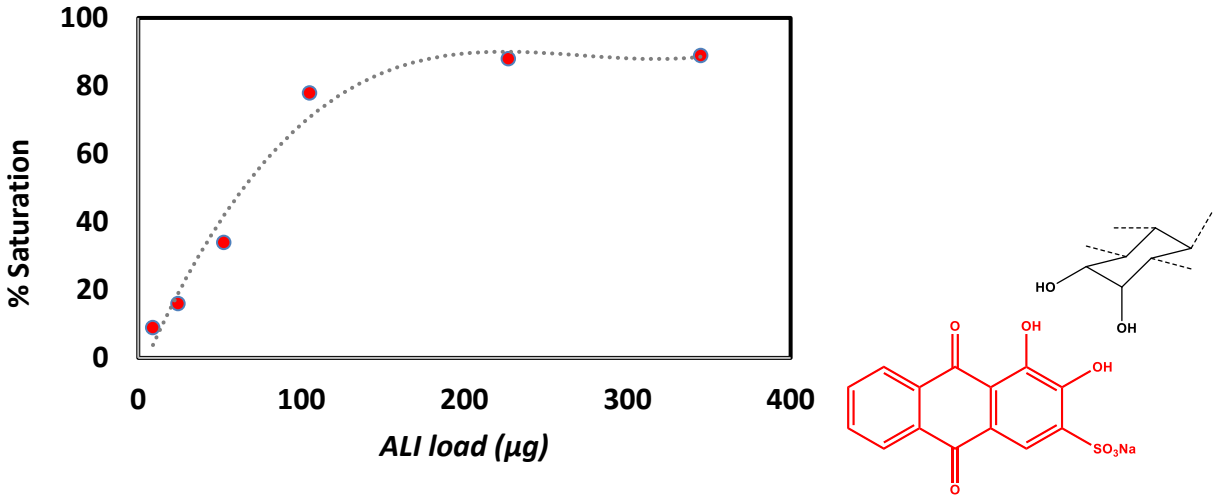

Figure S18| Saturation % curve defined using different loads of Alizarin Red S towards the same amount of living Chlorella cells. Absorbances have been evaluated at 522 nm after 24 hours of incubation and investigating the supernatants with and without living cells.

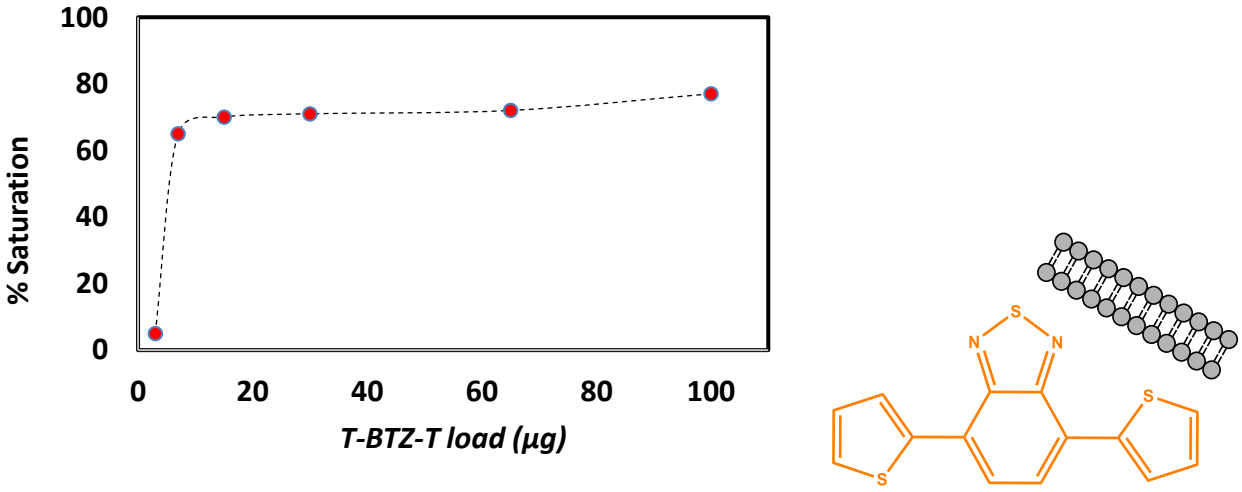

Figure S19| Saturation % curve defined using different loads of T-BTZ-T dye towards the same amount of living Chlorella cells. Absorbances have been evaluated at 438 nm after 24 hours of incubation and investigating the supernatants with and without living cells.

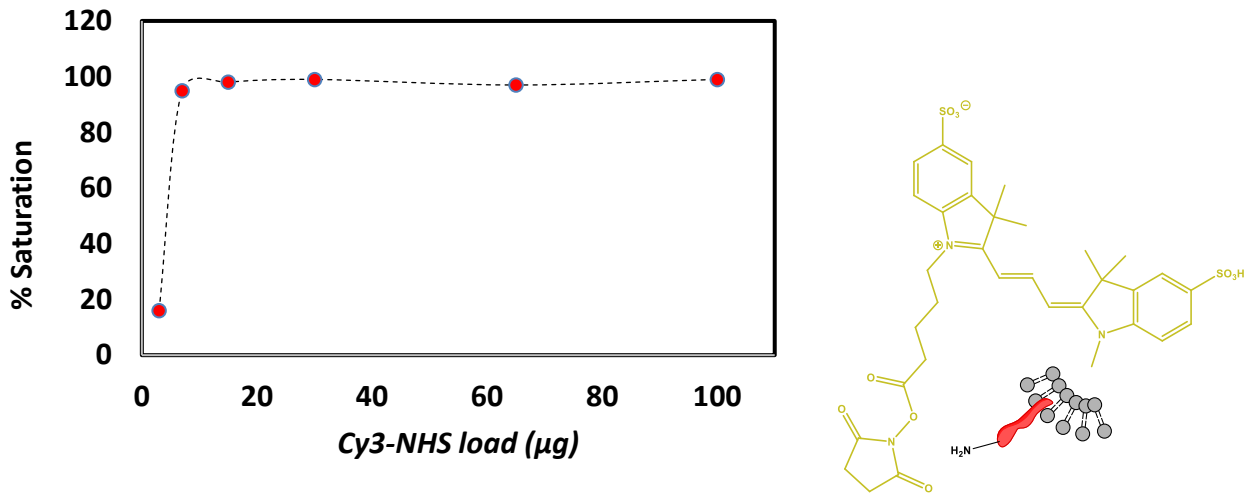

Figure S20| Saturation % curve defined using different loads of Cy3-NHS dye towards the same amount of living Chlorella cells. Absorbances have been evaluated at 516 nm after 24 hours of incubation and investigating the supernatants with and without living cells.

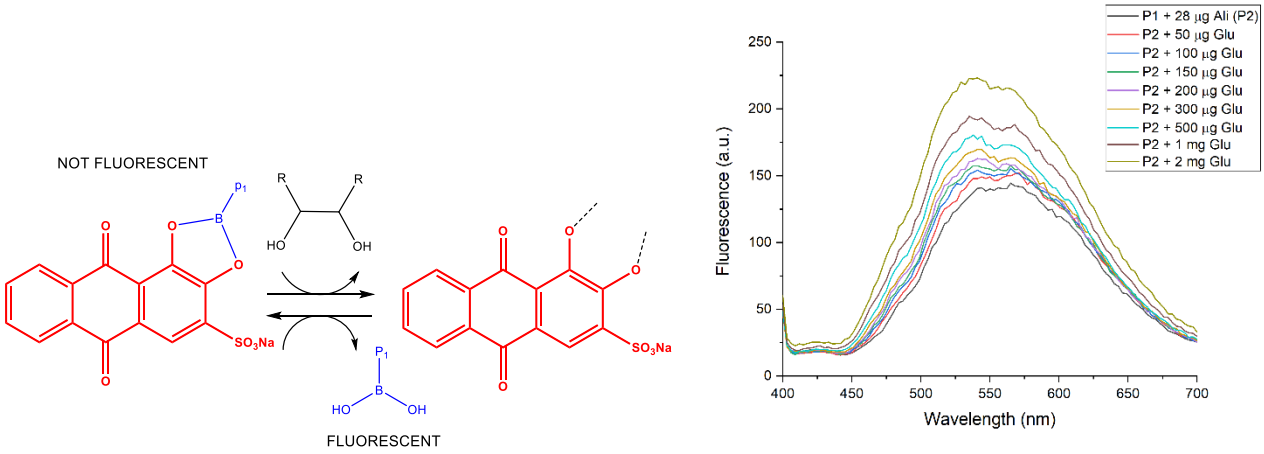

Step 1: kinetics of polymer delivery

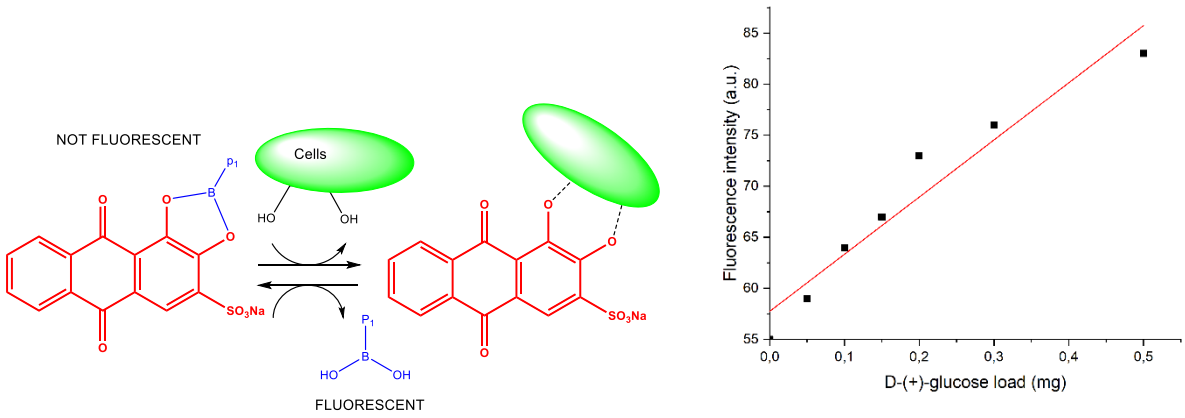

Step 2: interpolation by incubating living cells carrying sugar moeties

Figure S21| Displacement test performed for PDA-APBa and Alizarin Red S.

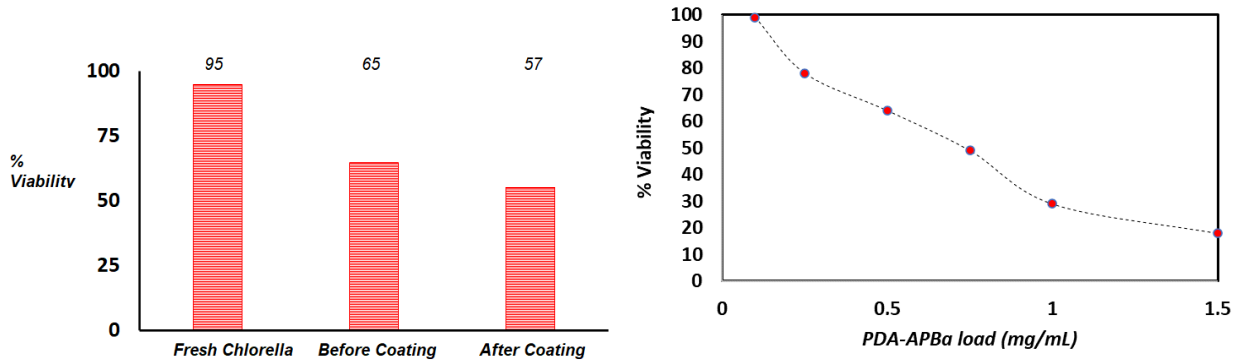

Figure S22| (right) Viability evaluation of living *Chlorella* cells *via* cytometric response. (left) Evaluation of IC50 value for PDA-APBa after exposition with living Chlorella cells and incubation with viability staining agent fluorescein diacetate (2h, 0.5 mg/mL of FDA). Viability refers to the maximal value exhibited by uncoated cells, and all the measures were spectrofluorimetrically detected (λexc.: 488 nm; λem.: 521 nm). IC50 value for PDA-APBa was defined as 0.79 mg/mL.

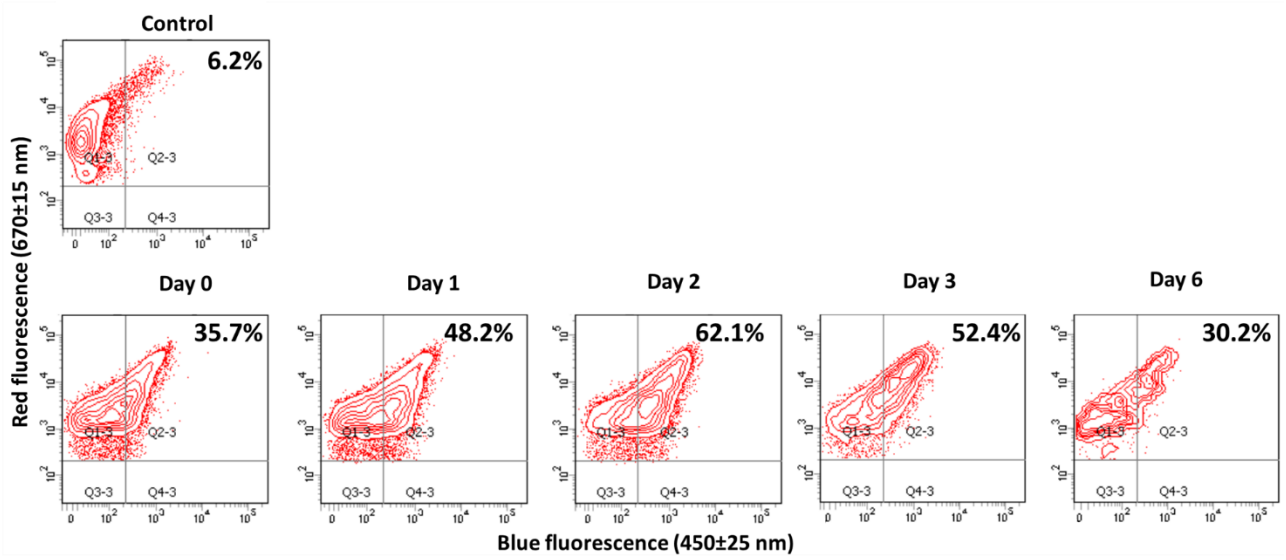

Figure S23| Artificial inheritance study of PDA-APBa coating on living *Chlorella* cells by flowcytometry. On the top, control experiment with uncoated bare and living *Chlorella* cells. On the bottom, PDA-APBa coated living Chlorella cells analyzed for several days. 10000 cellular events were recorded for each acquisition time, interpolating the red fluorescence values, related to chloroplast auto-fluorescence of living cells, versus blue fluorescence values, related to the PDA-APBa coating on living *Chlorella* cells.

The table reports concentration, standard deviation (SD, n=3) and relative standard deviation (RSD) of the elements of interest detected through TXRF in 7 10^6 bare and p1 coated *Chlorella vulgaris* cells. For each element,

concentration values with different letters are statistically different according to *t*-test ($p<0.01$); furthermore, except for K and Mn, element concentrations in bare Chlorella v. (not coated) and PDA-APBa coated living cells, are always statistically different for $p<0.05$. In CHV samples, Si and Br were below the limit of quantification (LoQ: Br, 0.005 mg/L; Si, 1.4 mg/L).

	Bare *Chlorella*			PDA-APBa		
Element	Conc.	SD	RSD	Conc.	SD	RSD
	µg / 7 10^6 cells		%	µg / 7 10^6 cells		%
Si	<LoQ			2.734	0.160	7.5
S	0.890 a	0.203	22.7	1.333 a	0.067	6.5
Cl	0.784 a	0.458	58.4	4.152 b	0.187	5.8
K	0.270 a	0.040	14.9	0.241 a	0.022	12.0
Ca	0.356 a	0.052	14.6	0.688 b	0.079	14.7
Fe	0.034 a	0.002	6.4	0.280 b	0.004	1.8
	ng / 7 10^6 cells		%	ng / 7 10^6 cells		%
Mn	2.4 a	0.3	12.2	2.9 a	0.3	11.3
Ni	1.3 a	0.2	14.3	2.4 a	0.4	22.7
Cu	2.9 a	0.8	28.9	5.0 a	0.6	14.3
Zn	11.4 a	0.8	7.3	23.4 b	2.6	14.1
Br	<LoQ			6.8	0.2	4.4

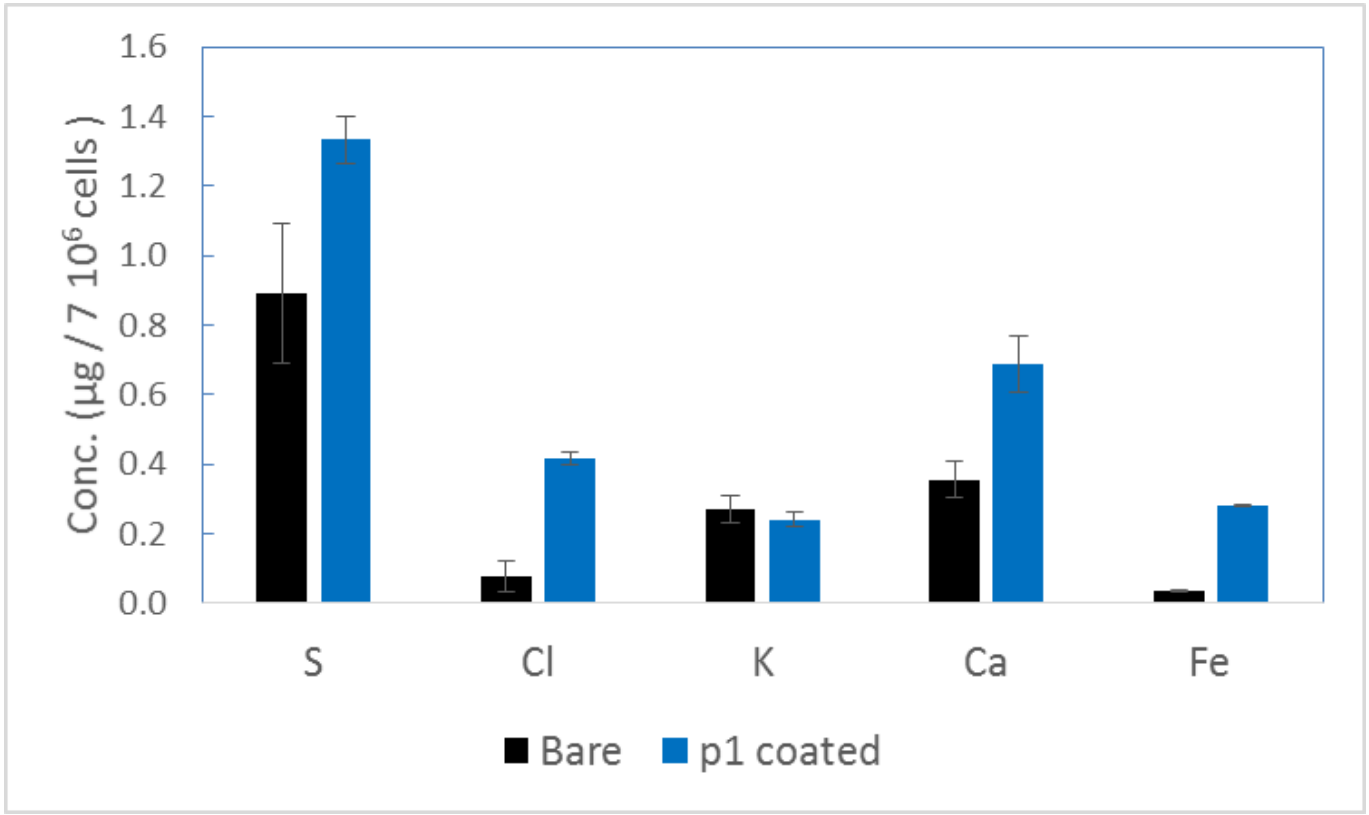

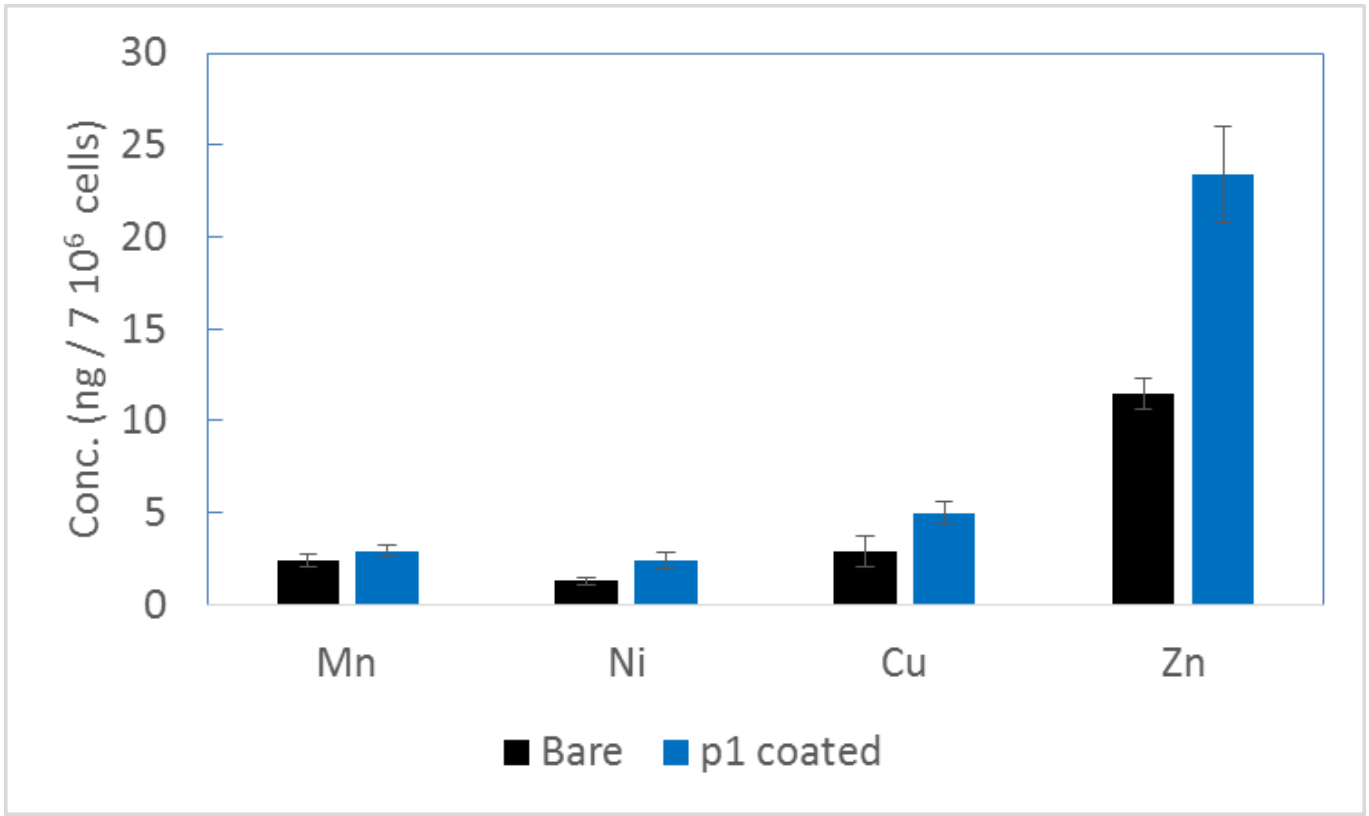

Figure S24| Table and histograms reporting TXRF analysis results.